AD-A038 792 TEXAS INSTRUMENTS INC DALLAS CENTRAL RESEARCH LABS F/G 20/5
MONOLITHIC LASER.(U)
MAR 77 K L LAWLEY, D W BELLAVANCE N00014-73-C-0288
UNCLASSIFIED TI-08-77-12 NL

| OF |
AD
A038792

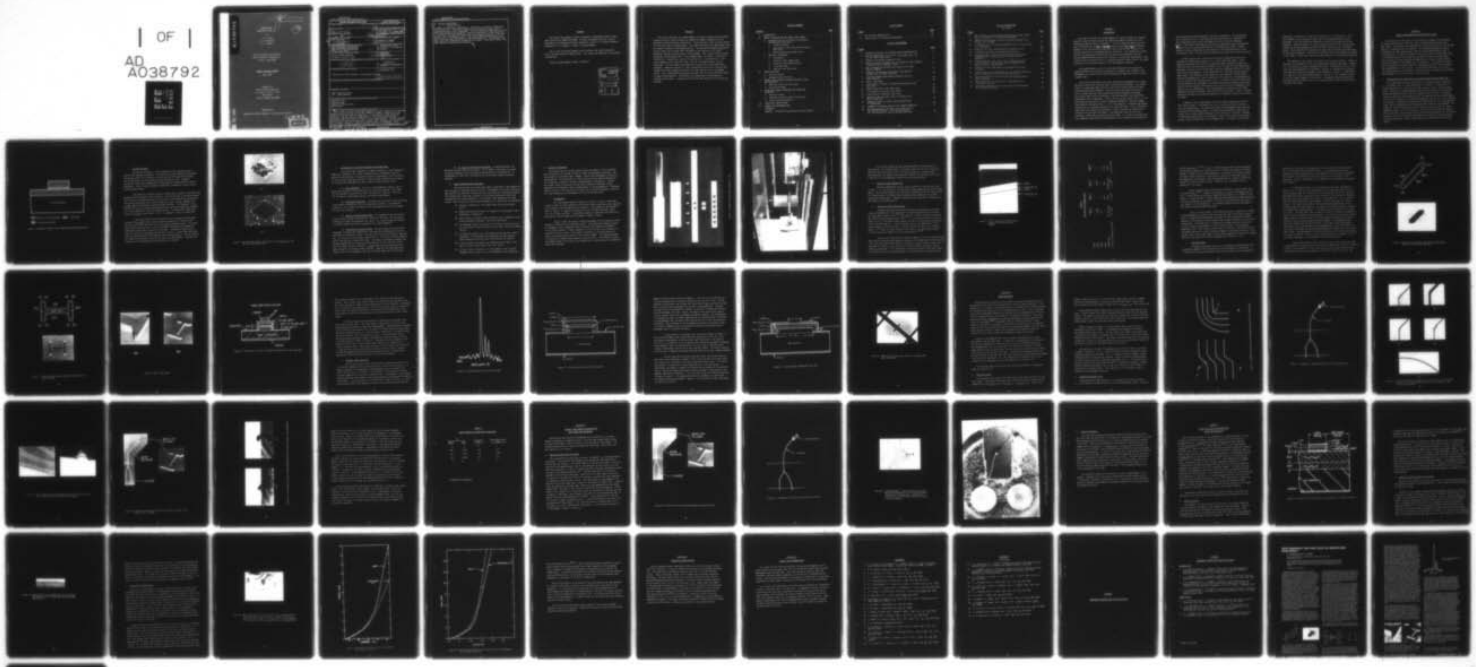

END

DATE
FILMED
5-77

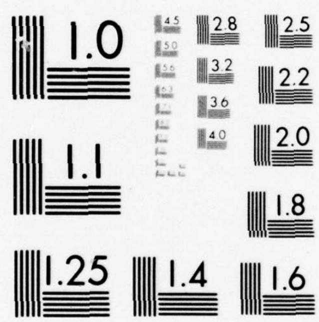

MICROCOPY RESOLUTION TEST CHART

NATIONAL BUREAU OF STANDARDS-1963-A

AD

12

UNCLASSIFIED
MONOLITHIC LASER (U)

by

K. L. Lawley
D. W. Bellavance
J. C. Campbell

Texas Instruments Incorporated
Central Research Laboratories
Dallas, Texas 75222

ANNUAL TECHNICAL REPORT

March 1977

Prepared for
Office of Naval Research
Arlington, Virginia 22217
NR 215-220
Contract N00014-73-C-0288

UNCLASSIFIED

Approved for Public Release - Distribution Unlimited

UNCLASSIFIED

SECURITY CLASSIFICATION OF THIS PAGE *(When Data Entered)*

REPORT DOCUMENTATION PAGE

READ INSTRUCTIONS BEFORE COMPLETING FORM

1. REPORT NUMBER

2. GOVT ACCESSION NO.

3. RECIPIENT'S CATALOG NUMBER

4. TITLE *(and Subtitle)*

MONOLITHIC LASER (U)

5. TYPE OF REPORT & PERIOD COVERED

Annual Technical rept. no. 3
1 May 1975 - 31 January 1977

6. PERFORMING ORG. REPORT NUMBER

TI-08-77-12

7. AUTHOR(s)

W. L. Lawley
D. W. Bellavance
J. C. Campbell

8. CONTRACT OR GRANT NUMBER(s)

N00014-73-C-0288

9. PERFORMING ORGANIZATION NAME AND ADDRESS

Texas Instruments Incorporated
Central Research Laboratories
13500 North Central Expressway
Dallas, Texas 75222

10. PROGRAM ELEMENT, PROJECT, TASK AREA & WORK UNIT NUMBERS

PE 61153N-14, RF 41-423-001,
NR 215-220

11. CONTROLLING OFFICE NAME AND ADDRESS

Office of Naval Research
Arlington, Virginia 22217

12. REPORT DATE

March 1977

13. NUMBER OF PAGES

60

14. MONITORING AGENCY NAME & ADDRESS *(if different from Controlling Office)*

69p.

15. SECURITY CLASS. *(of this report)*

UNCLASSIFIED

15a. DECLASSIFICATION/DOWNGRADING SCHEDULE

16. DISTRIBUTION STATEMENT *(of this Report)*

FH1423

Approved for Public Release - Distribution Unlimited

RFH1423001

17. DISTRIBUTION STATEMENT *(of the abstract entered in Block 20, if different from Report)*

18. SUPPLEMENTARY NOTES

ONR Scientific Officer
Tel: (202) 692-4411

19. KEY WORDS *(Continue on reverse side if necessary and identify by block number)*

Monolithic Laser
Injection Laser
Integrated Optical Source
Surface Laser

20. ABSTRACT *(Continue on reverse side if necessary and identify by block number)*

This report describes the accomplishments of the third phase of the research program carried out under Contract No. N00014-73-C-0288 to develop the first prototype integrated optical transmitter. A new monolithic laser structure called an I-bar mesa laser was demonstrated. This double heterojunction GaAs/GaAlAs laser was grown by selective liquid phase epitaxy. The best devices operated at 525 mA drive current with a pulsed, 300 K threshold current density of 7.5 kA/cm^2. Methods of fabricating these devices are discussed. Also, various types of grown waveguides including bends and Y's were demonstrated.

DD FORM 1 JAN 73 1473 EDITION OF 1 NOV 65 IS OBSOLETE

UNCLASSIFIED

SECURITY CLASSIFICATION OF THIS PAGE *(When Data Entered)*

20. Abstract (Continued)

For bends, a 3 dB signal attenuation is observed at a radius of curvature of ~ 1.3 mm (50 mils). This radius appears to be a practical lower limit for integrated optical circuit waveguides. The I-bar mesas were combined on a chip with a grown three-layer waveguide. Measured intensity of light transmitted by end-firing from the laser through the curved waveguide was 35% of the laser emission with a narrowband output. Also, etched double heterojunction mesa laser structures were fabricated on underlying waveguides. The emission from these lasers was evanescently coupled to this guide. A coupling of 25% of the laser emission to the guide was observed.

Foreword

This report was prepared by Texas Instruments Incorporated, Dallas, Texas, under Contract No. N00014-73-C-0288. At Texas Instruments the work is being performed in the Advanced Technology Laboratory, a part of TI's Central Research Laboratories. Dr. Kenneth L. Lawley is Program Manager.

This is the third Annual Report on this contract and covers the period from 1 May 1975 through 31 January 1977. This report was submitted by the authors in March 1977.

Texas Instruments report number is 08-77-12.

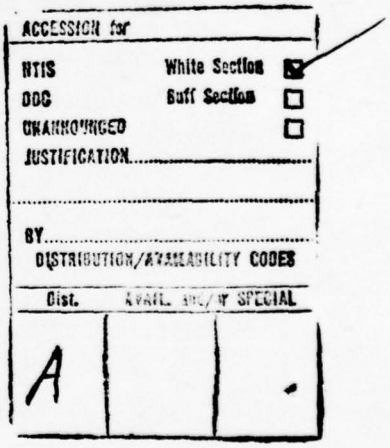

Abstract

This report describes the accomplishments of the third phase of the research program carried out under Contract No. N00014-73-C-0288 to develop the first prototype integrated optical transmitter. A new monolithic laser structure called an I-bar mesa laser was demonstrated. This double heterojunction GaAs/GaAℓAs laser was grown by selective liquid phase epitaxy. The best devices operated at 525 mA drive current with a pulsed, 300 K threshold current density of 7.5 kA/cm^2. Methods of fabricating these devices are discussed. Also, various types of grown waveguides including bends and Y's were demonstrated. For bends, a 3 dB signal attenuation is observed at a radius of curvature of $\sim$ 1.3 mm (50 mils). This radius appears to be a practical lower limit for integrated optical circuit waveguides. The I-bar mesas were combined on a chip with a grown three-layer waveguide. Measured intensity of light transmitted by end-firing from the laser through the curved waveguide was 35% of the laser emission with a narrowband output. Also, etched double heterojunction mesa laser structures were fabricated on underlying waveguides. The emission from these lasers was evanescently coupled to this guide. A coupling of 25% of the laser emission to the guide was observed.

TABLE OF CONTENTS

LIST OF TABLES

LIST OF ILLUSTRATIONS

LIST OF ILLUSTRATIONS

(Continued)

SECTION I

INTRODUCTION

This report describes the accomplishments of the third phase of a research program carried out under Contract No. N00014-73-C-0288 to develop the first prototype integrated optical transmitter. The third phase has been a continuation of materials and device development in GaAs, (Ga,In)As, and (Ga,Aℓ)As with emphasis on the fabrication of monolithic laser structure that serves as the radiation source on an integrated optical transmitter. The integration of laser sources with waveguides and modulators currently being developed under ONR Contract N00014-75-C-0501 need not be limited to a transmitter application. Such circuits could find future utility in spectrum analysis, optical logic, and signal processing in the infrared region of the electromagnetic spectrum.

The accomplishments of the first and second phases of this program are summarized below to illustrate the evolution of concepts that resulted in the development of a pulsed, 300 K double heterojunction monolithic laser structure in phase three.

During the initial phase, the effort involved the development of a unique (Ga,In)As surface laser and high index infrared glass waveguides. The surface laser is a vapor-grown mesa structure with vertical grown crystalline facets furnishing the optical feedback. The structure can be placed and grown at will on a GaAs substrate using conventional photolithographic techniques. This unique laser structure represents a radical departure from conventional semiconductor laser technology. Ternary alloy $Ga_{1-x}In_xAs$ mesas with $0 < x < 0.2$ were grown and the details of their morphology determined. Optically pumped laser emission from mesas with $0 < x < 0.1$ was observed. Threshold pump powers, efficiencies, and emission characteristics were determined. Also, a GaAs mesa diode laser was successfully fabricated. The p-n junction was formed by Zn diffusion into the top of the mesas. The diode mesa laser was the first monolithic, nondiscrete injection laser ever made. It is the first diode laser ever completely fabricated (including optical cavity formation) monolithically

using conventional photolithographic fabrication technology. This development was a significant first in semiconductor laser technology with importance in both integrated optical source development and discrete laser technology. Finally, high quality chalcogenide glass optical waveguides were also developed. Losses as low as 0.4 dB/cm were measured in sputtered As_2S_3 films. Channel optical stripline waveguides were fabricated by overlaying photoresist strips on the glass films. Low-loss channel waveguiding was observed in these structures.

In phase two the work of phase one on optically pumped mesa lasers was extended to developing $Ga_{1-x}In_xAs$ ($0 \leq x \leq 0.06$) diode mesa lasers. These homojunction devices were the first wavelength-tunable, monolithic electrical injection lasers and were operated between liquid nitrogen and room temperatures. Monolithic arrays of up to six GaAs mesa lasers were operated with all the lasers oscillating simultaneously. Laser characteristics, including emission spectra, power output, and threshold current densities, were measured. Because these devices are homojunctions, their threshold current densities at room temperature are very high and their efficiencies are low. To improve on these characteristics work was begun on the development of single-heterostructure GaAs-$Ga_{1-x}Al_xAs$ mesa lasers that would operate under pulsed drive currents with low threshold current densities at room temperature. Their development and integration with planar waveguides continued into phase three of the current contract. Finally, chemical etching of the mesa structures were explored as a possible alternative to growing the mesas.

A summary of the accomplishment of the third phase presented in detail in this report follows. A new monolithic laser structure called an I-bar mesa laser was demonstrated. This double heterojunction GaAs/GaAlAs laser was grown by selective liquid phase epitaxy. The best devices operated at 525 mA drive current with a pulsed, 300 K threshold current density of 7.5 kA/cm^2. Methods of fabricating these devices are discussed. Also, various types of grown waveguides, including bends and Y's, were demonstrated. For bends, a 3 dB signal

attenuation is observed at a radius of curvature of ~ 1.3 mm (50 mils). This radius appears to be a practical lower limit for integrated optical circuit waveguides. The I-bar mesas were combined on a chip with a grown three-layer waveguide. Measured intensity of light transmitted by end-firing from the laser through the curved waveguide was 35% of the laser emission with a narrowband output. Also, etched double heterojunction mesa laser structures were fabricated on underlying waveguides. The emission from these lasers was evanescently coupled to this guide. A coupling of 25% of the laser emission to the guide was observed.

The remainder of this report is divided into five major sections. Section II describes the development of the I-bar double heterojunction mesa laser. Section III is a discussion of grown waveguides and bends. The combination of the I-bar laser and grown waveguides is presented in Section IV, followed by a discussion of etched mesa lasers and evanescent field coupling in Section V. Some preliminary results on contacting methods appear in Section VI, and a summary of Phase III of this project appears in Section VII. An appendix containing pertinent published journal articles and a list of presentations resulting from this work concludes this report.

SECTION II

DOUBLE HETEROJUNCTION GaAs-GaAℓAs MESA LASERS

During this year, the thrust of the program was changed from development of single heterostructure (SH) mesa lasers to double heterostructure (DH) mesa lasers. The SH mesa laser represented an intermediate stage in the development of a prototype optical transmitter. This approach combined the latest developments of vapor phase epitaxy (VPE) and liquid phase epitaxy (LPE) in a hybrid device. At Texas Instruments a new mesa structure was developed under a TI-funded program for the selective LPE growth of monolithic mesa lasers. This new mesa structure presented the opportunity to work on advanced device structures capable of room temperature, cw operation. The successful development and operation of DH mesa lasers at room temperature was a major milestone and accomplishment in this program. The following subsections will discuss the considerations for the choice of the DH mesa laser, the materials technology and development of the DH mesa laser, and DH devices.

A. Considerations for the Choice of the Double Heterojunction Mesa Laser

The single heterostructure mesa laser is a prototype optical transmitter in its simplest form. As shown conceptually in Figure 1, it consists of a single heterostructure injection mesa laser grown on top of a (Ga,Aℓ)As waveguide. Radiation is coupled downward from the active region into the passive (Ga,Aℓ)As waveguide and continues to propagate across the chip. The device structure requires a unique combination of two separate materials technologies: (1) LPE for the growth of the (Ga,Aℓ)As waveguides, and (2) VPE for the formation of the mesas. Although each technology has been successful in its own applications, the two technologies have been marginally successful when combined. For simplicity the materials problems can be broken into three broad, but interdependent, areas: (1) the LPE growth of (Ga,Aℓ)As, which is both an integral part of the laser structure and serves as the optical waveguide; (2) the LPE-VPE interface; and (3) the growth of high-quality VPE mesas for the laser cavity on the LPE (Ga,Aℓ)As. Each of these subjects was discussed in the previous report.[1]

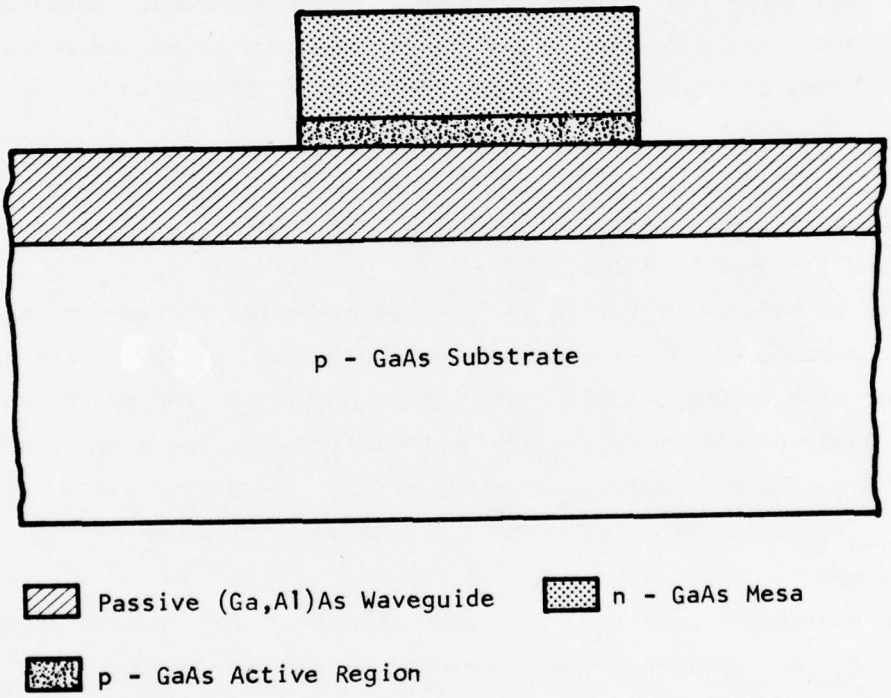

Figure 1 Conceptual Diagram of the Coupled Laser-Waveguide Device

1. LPE-VPE Interface

The LPE-VPE interface is the key problem in this structure since it controls many important processes: (1) electrical contact between the substrate and the mesa laser, (2) diffusion of the Zn from the LPE layer into the mesa, and (3) the quality of the surface on which the mesa is grown. Unwanted interfacial layers could degrade any of these important areas and affect device performance. Many of these problems are enhanced by attempting to use a hybrid LPE-VPE growth process.

The effect of interfacial layers is particularly evident in the electrical properties and the growth of the VPE mesa.[1] The difficulties in the device design were found to be related primarily to limitations in the processing, particularly the cleaning procedures that could be effectively used. Neither chemical nor in situ vapor etch techniques alleviated these problems. The presence of Aℓ in the top LPE layer particularly degraded materials and device properties, probably due to the formation of insoluble aluminum oxides. No high quality mesas were grown on $Ga_{1-x}Al_xAs$ layers with $x \geq 0.01$. An example is shown in Figure 2(a).

To overcome the difficulties encountered in the growth of GaAs mesas directly on $Ga_{1-x}Al_xAs$ layers, the structure was modified to include a thin LPE GaAs buffer layer that overlies the $Ga_{1-x}Al_xAs$ waveguide layers. The buffer layer must be kept very thin ($\leq$ 1 μm) to minimize the separation between the heterojunction and the p-n junction in the mesa. High-quality mesas such as shown in Figure 2(b) have been grown on this structure. Devices have been made with this structure where the waveguide layer was $Ga_{0.8}Al_{0.2}As$. The p-n junction was formed by diffusing Zn from the LPE layer into the VPE mesa. These devices lased at 77 K with threshold current densities $\leq$ 10 kA/cm^2.

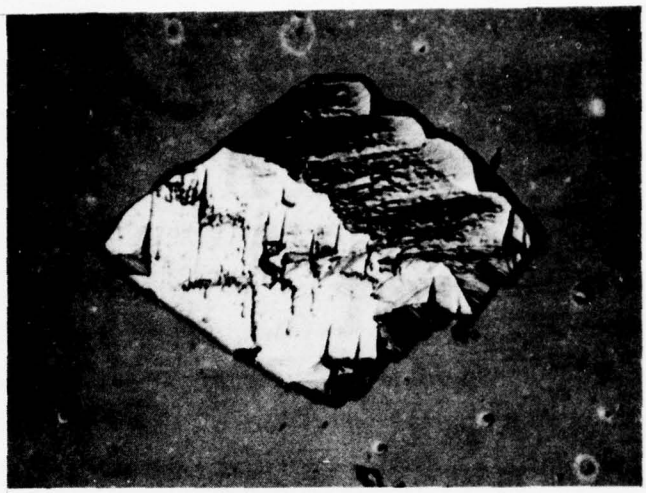

(a)

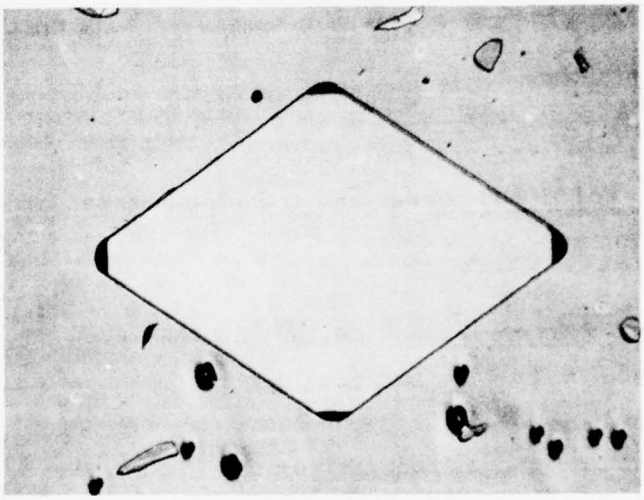

(b)

Figure 2 VPE GaAs Mesas Grown (a) Directly on $Ga_{0.85}Al_{0.15}As$, and (b) on a GaAs Buffer Layer

2. Limitations of the Single Heterostructure Mesa Laser

The SH mesa laser represents a simple prototype of a room temperature, monolithic transmitter and is best considered as an intermediate step to a practical working device. During the course of investigation, the limitations of this structure have been clarified. Some of these limitations are related to the materials technology and some are basic to the structure itself.

(1) High Thresholds. The SH is a room temperature device, but by nature has relatively high threshold current densities compared to DH lasers. For low threshold cw operation at 300 K, DH lasers are required. These can only be grown by liquid phase epitaxy or molecular beam epitaxy.

(2) Substrate Orientation. The mesas must be grown on {110} substrates to be properly oriented for vertical faceting of the mesas. The waveguide studies are all on {100} substrates and the electrooptic effects are strongest for the ⟨110⟩ directions.

(3) Doping in the Waveguide Layer. The waveguide layer also serves as the diffusion source to form the p-n junction in the mesa. The very heavy Zn doping will make the waveguides very lossy. All current waveguide research is directed towards low carrier concentration, n-type waveguides.

(4) LPE-VPE Hybrid Growth System. VPE mesa growth on LPE (Ga,Aℓ)As waveguides introduces many problems for the materials technology which can be attributed to interfacial layers. The major difficulties as previously reported[1] are: (1) erratic current-voltage characteristics, (2) erratic diffusion behavior, and (3) the need for a GaAs buffer layer. The latter requirement increases the distance between the p-n junction and the heterojunction in the laser cavity and will affect the laser threshold. In situ vapor etch techniques have not been successful in overcoming these problems. Chemical etch techniques often create a hole in the waveguide layer that introduces additional difficulties.

(5) P-n Junction Formation by Diffusion. As mentioned above, the diffusion behavior tends to be erratic. The Zn dopant is difficult to contain and control because of its high vaporization pressure and high mobility. Zn contamination of the top of the mesa during the diffusion causes processing problems.

3. Double Heterojunction Mesa Laser

The SH mesa laser was a major step toward a monolithic, room temperature laser source for integrated optical circuits. Development work on this structure has clarified the technical difficulties with this design as indicated previously. The DH mesa laser, described in detail in the following sections, clearly has the potential of being a monolithic, low threshold, room temperature cw laser source. The new structure offers many advantages and in particular the following:

(1) The mesa is monolithic, with grown facets forming the optical cavity.

(2) Double heterostructure lasers are capable of low threshold, room temperature, cw operation.

(3) The structure is grown on {100} substrates and is compatible with present waveguide, modulator, and switch technology.

(4) The waveguide layers are not part of the laser structure and are not restricted in their structure, carrier type, or carrier concentration.

(5) All materials growth is by liquid phase epitaxy and not a hybrid technology. The techniques are compatible with the low-cost batch processing currently used in the electronics industry.

(6) Since the lasers can operate cw, modulation can be done in the optical circuit rather than at the laser source.

(7) The laser cavity is grown in a stripe geometry with a totally embedded active region for very low threshold current operation.

B. Materials Technology

Liquid phase epitaxy has been used at Texas Instruments in the integrated optics program for the growth of both DH lasers and waveguide structures. The realization of the DH mesa laser, however, required the development of selective LPE technology. The guidelines for selective LPE have now been established at TI and applied to growth in various crystallographic orientations. I-bar DH mesa lasers grown by selective LPE have been successfully operated at room temperature and represent a major accomplishment in the development of integrated optical circuits. This section will discuss the LPE growth parameters, selective LPE, mesa morphology, and development of the I-bar DH mesa laser.

1. LPE Reactors

The liquid phase epitaxial reactors currently in use at TI have been refined to meet the high standards of controlled uniform submicron layers required in the growth of low threshold DH laser material. The graphite slider assembly shown in Figure 3 is capable of growing up to six different epitaxial layers on a 2.5 cm^2 GaAs substrate. The graphite assembly is machined from high purity, high density DFP-3-2 graphite (Poco Graphite, Decatur, Texas).

Figure 4 shows the reactor furnace and chamber with the graphite slider assembly in position for an epitaxial growth. The three-zone Lindberg furnaces are equipped with an isothermal liner to minimize the temperature gradients in the slider assembly. Typical gradients of 2 to 3°C over a 16 cm length are achieved with this system. The furnace is mounted on a rolling platform to permit rapid heating and cooling of the reaction chamber. The reaction chamber is continually flushed during growth with H_2 purified in a Pd diffusion furnace. The oxygen content of the input H_2 and exhaust gas is monitored with a Panametrics Model 2000 hygrometer.

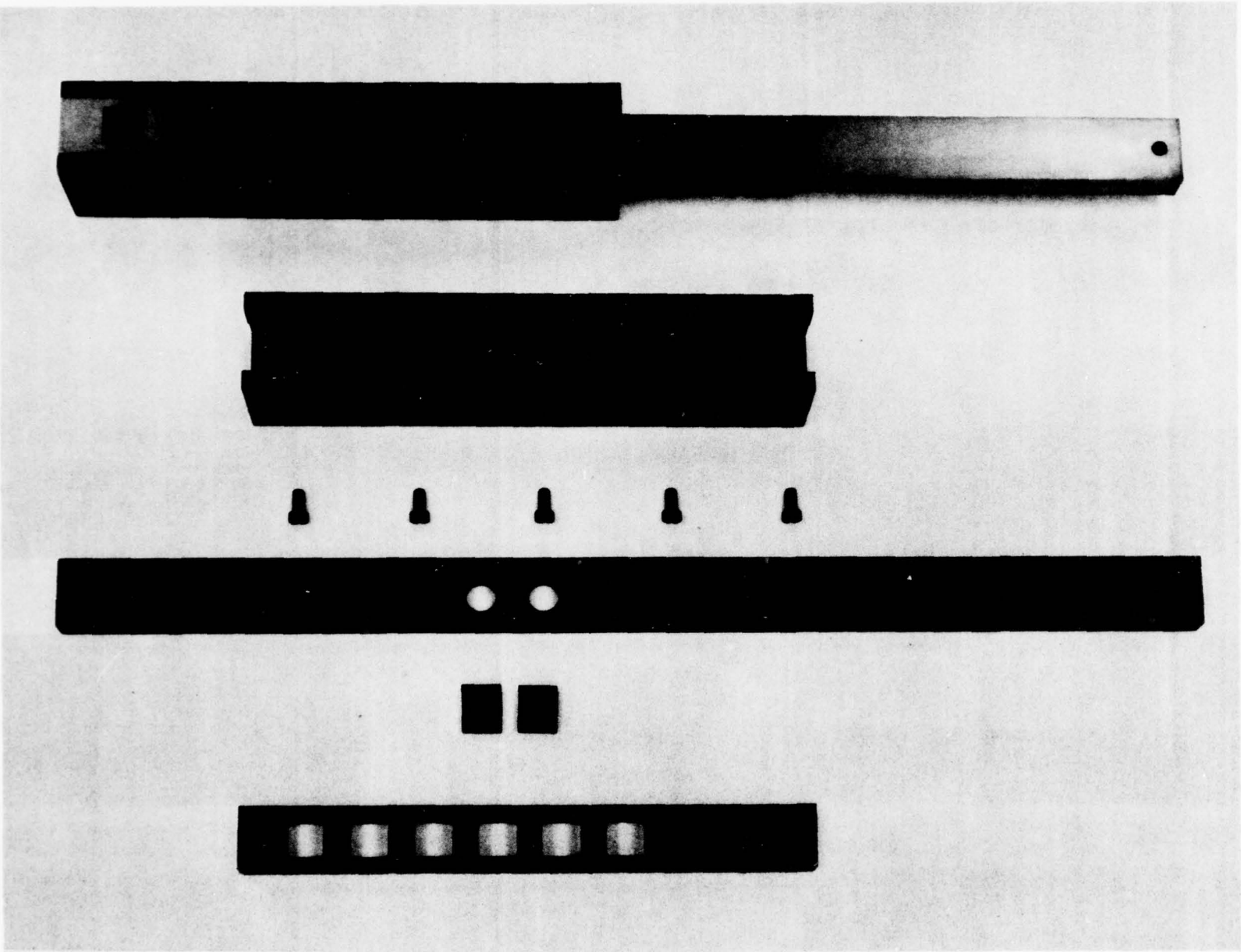

Figure 3 Graphite Sliding Boat Assembly for LPE

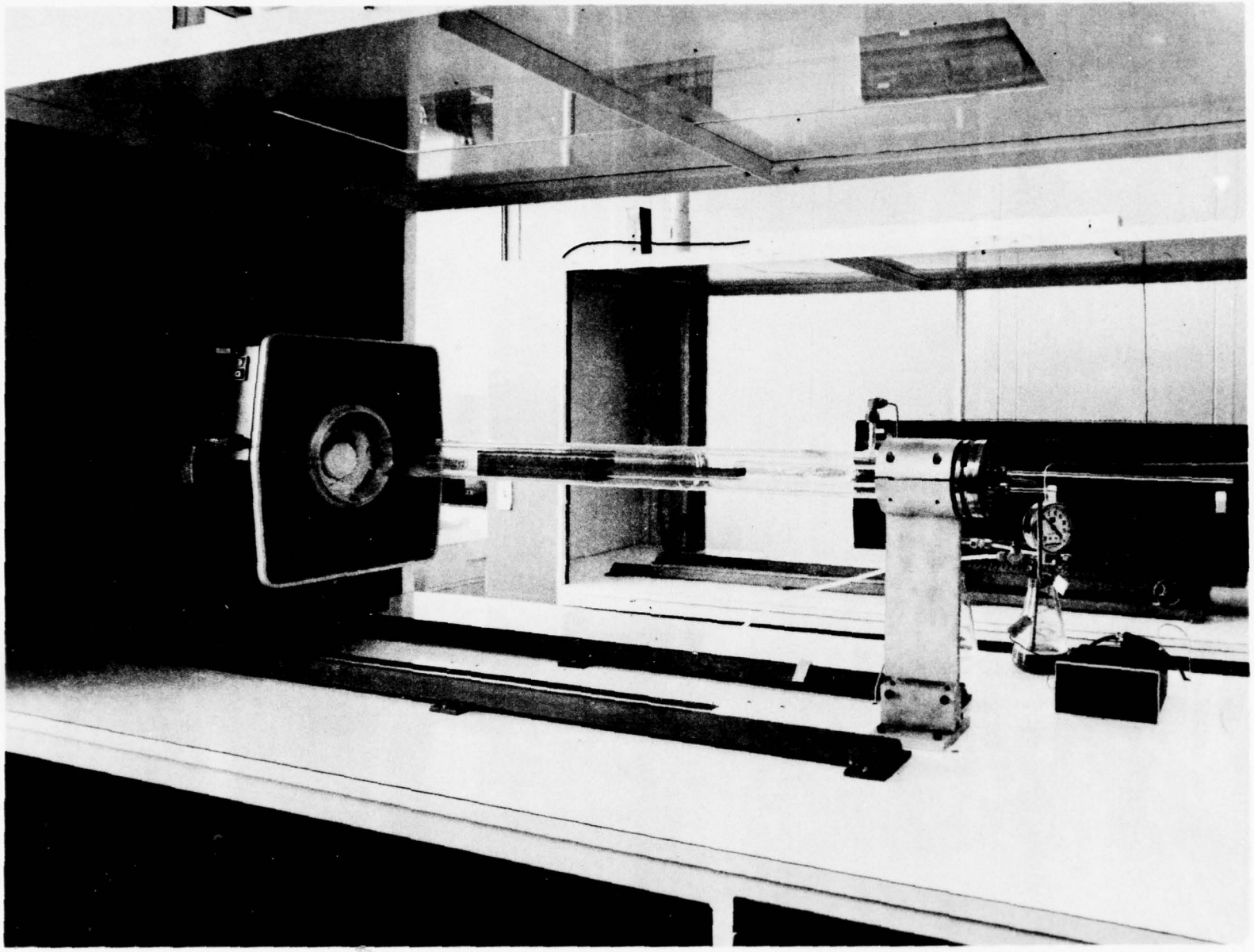

Figure 4 Reactor Furnace and Chamber with the Graphite Slider Assembly in Position for an Epitaxial Growth

This reactor system has been used extensively in the growth of DH laser material for discrete lasers. Epitaxial layers 0.1 to 0.2 μm thick are routinely grown (see Figure 5) for this device structure. Discrete lasers fabricated from this material have measured threshold current densities as low as 585 A/cm^2 at room temperature under 200 ns pulsed conditions.

2. Epitaxial Layer Compositions

The melt compositions used to grow a typical DH I-bar mesa are given in Table I. In this system, Sn is used as the n-type dopant and Ge as the p-type dopant. The Aℓ concentrations were verified by growing a series of single layers for standardization and determining the actual grown composition from photoluminescence measurements. The melt compositions for the carrier concentrations were based on published data.[2-7]

3. Selective Liquid Phase Epitaxy

Although there have been several extensive investigations of growth rates and morphologies of III-V materials in selected patterns and directions for vapor phase epitaxy (VPE),[8-12] there was very limited information available for selective liquid phase epitaxy (LPE).[13,14] During the course of this work, Samid, et al.,[15] published further work on the use of stripes grown by selective LPE for discrete devices. In some instances, such as the dominance of {111} facets along the ⟨110⟩ substrates, selective VPE and LPE behave in a similar manner.[11,15] Quite different growth occurs, however, for LPE diamond mesas[16] on (110) substrates compared with VPE diamond mesas.[1,17,18]

There are two significant limitations inherent in the LPE growth process that must be recognized when comparing selective VPE technology with selective LPE. First, VPE has an additional degree of freedom in the wide range of Ga/As ratios available for growth. This ratio can be varied to affect the growth rate for different directions.[12] This phenomenon is possible because of the polar nature of the GaAs crystal and has been applied to grow new device structures such as

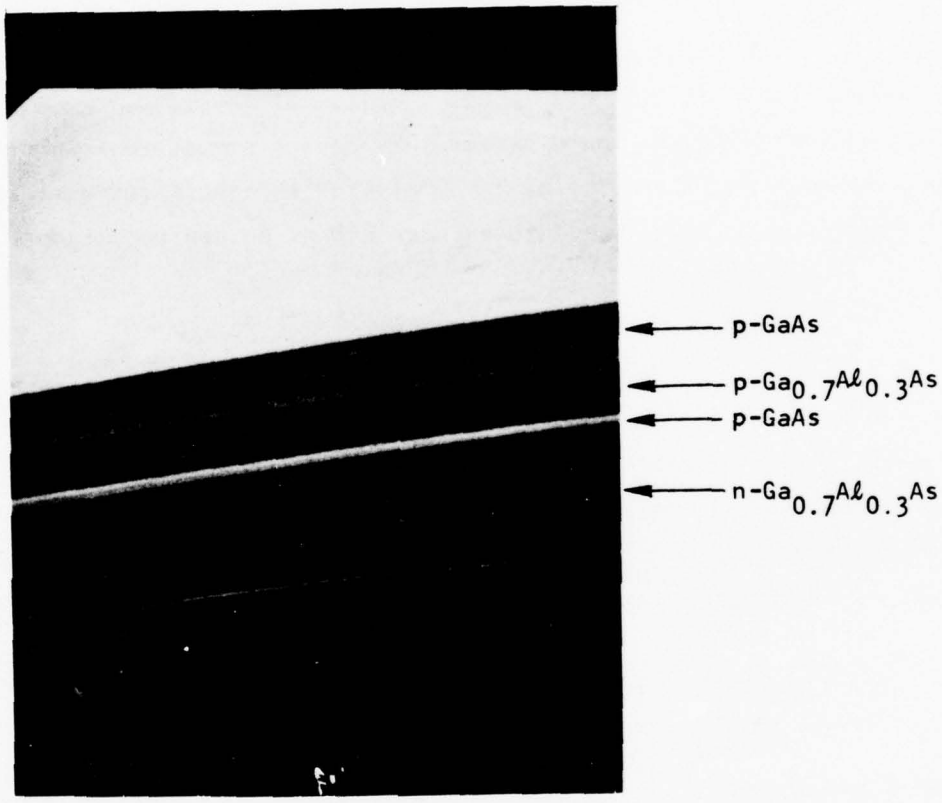

Figure 5 SEM of Cleaved and Stained Cross Section of DH Laser Material (6640X)

Table I

DH I-Bar Melt Compositions

	Layer 1	Layer 2	Layer 3	Layer 4
Ga(g)	2	2	2	2
Aℓ(g)	0.002	--	0.002	--
Sn(g)	0.6	--	--	--
Ge(g)	--	0.01	0.02	0.02
Composition	$Ga_{0.7}Al_{0.3}As$	GaAs	$Ga_{0.7}Al_{0.3}As$	GaAs
Carrier Concentration (cm^{-3})	8×10^{17}	1×10^{18}	1×10^{18}	3 to 5×10^{18}

the VPE mesa laser.[1,17,18] In LPE, a limited range of Ga/As ratios determined by the growth temperature is available only in the Ga-rich regime of the phase diagram. Second, the LPE growth mechanism is a diffusion rate limited process. To obtain uniform thickness in the epitaxial layers and avoid edge effects at the mask/growth area boundary, the growth geometries are limited to small mask widths[13] or narrow stripes (< 50 μm). Selective VPE is capable of 250 μm geometries[11] and larger.

Several types of mask materials were considered. Al_2O_3 has been used by several workers.[13,15] However, this material is difficult to deposit and to etch. Silicon oxide can be readily deposited and etched, but is soluble in the Ga melt. Silicon nitride is readily deposited and patterned by plasma techniques and is not dissolved by the Ga melt. Silicon nitride was used as the mask for all selective LPE investigations. All epitaxial depositions were performed in the reactor system previously described.

Prior to crystal growth, the polished substrate is coated with ~ 2000 Å of plasma-deposited silicon nitride for a mask and then with a layer of photoresist. Standard photolithographic techniques are used to define the pattern openings in the photoresist and plasma etching to open the pattern in the silicon nitride mask. The window area is cleaned with a common oxide etch just prior to resist removal and placement in the LPE growth system. Starting growth temperatures are ~ 735°C and the cooling rate is 0.2°C/min. The growth rate for the masked substrates is greatly enhanced compared to unmasked substrates. Slow cooling rates, short growth times, and low growth temperatures are used to improve control of the growth and to obtain reasonably thin layers (~ 1 μm).

4. I-Bar Mesa Laser

In designing new grown devices, it is necessary to consider both the limitations imposed by the LPE process and the requirements of the device. It is clear from the previous discussion that the LPE process limits the design to

working with (1) narrow stripe geometries and (2) naturally occurring facets (i.e., no manipulation of the Ga/As ratio). An IOC monolithic mesa laser requires (3) facets perpendicular to the substrate to provide optical feedback, (4) uniformly flat and parallel epitaxial layers, and (5) growth on {100} substrates. The last requirement is for compatibility with presently developed active devices.

It was observed early in the investigation and later confirmed by Samid, et al.,[15] that for {100} GaAs substrates, stripes grown parallel to the {110} cleavage planes have facets that are not perpendicular to the substrate. Rectangular structures would have similar features; this orientation, therefore, does not satisfy the perpendicular facets in requirement (3). For a rectangle with all sides along {100} planes, however, the structure shown in Figure 6 results. The resulting mesa has a flat top and facets perpendicular to the substrate along the long dimension. The ends with the short dimension, however, are dominated by nonperpendicular {111} facets, and the structure is not useful as a laser. The I-bar mesa laser, as shown in Figure 7, results from combining three of these rectangles into one structure. In this new structure the central member serves as the laser cavity, and the perpendicular facets at the ends of the laser cavity region provide the optical feedback. The nonperpendicular facets are removed from the central cavity to the ends of the cross members. The length of the cross members has been exaggerated in Figure 7 and must only satisfy the requirement of moving the nonperpendicular facets out of the central laser region. SEM photographs illustrating the high quality of as-grown facets are shown in Figure 8. Contrary to previous observations by Kawakami, et al.,[14] the growth morphology is not dependent on the Al concentration.

Double heterojunction lasers with the I-bar structure have been grown. A cross section illustrating layer structure and compositions is shown in Figure 9. Typical I-bar dimensions for the central laser cavity are 350 to 400 μm long, 25 μm wide; and for the cross members, 150 to 350 μm long, 25 μm wide. The

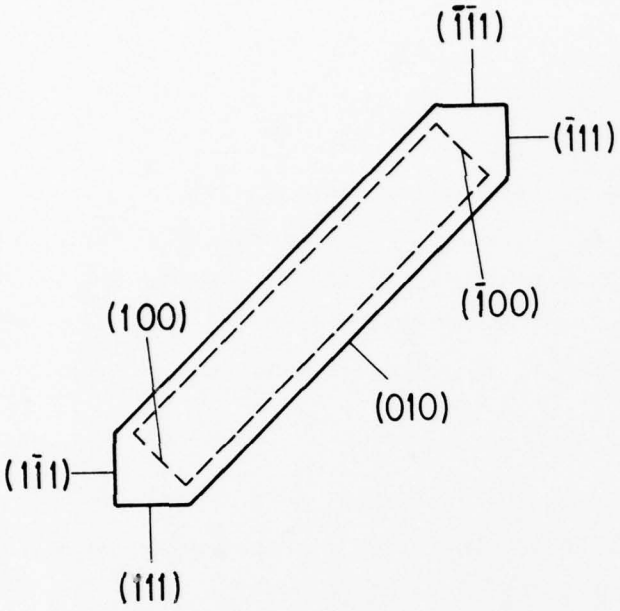

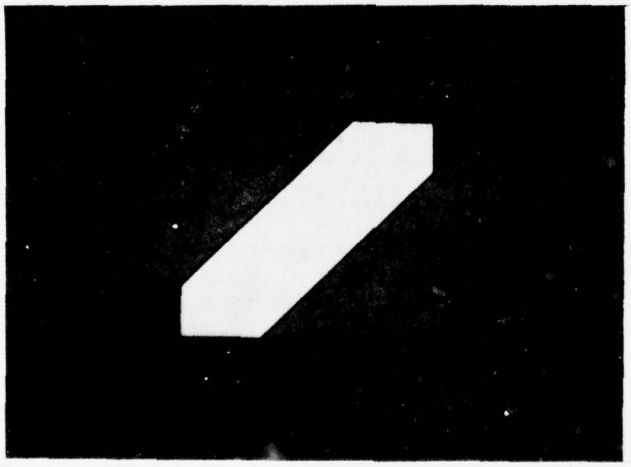

Figure 6 Selective LPE Rectangle Mesa Showing Mask Opening (dashed line) and Facet Formation

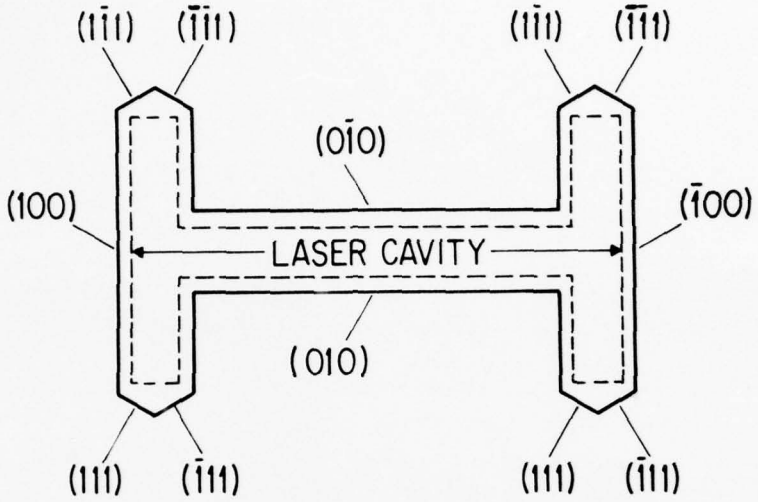

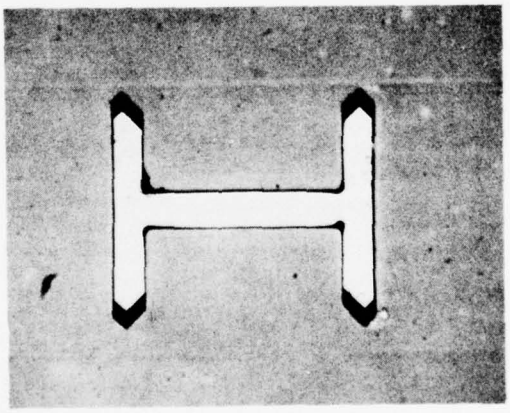

Figure 7 I-Bar Mesa Showing Mask Opening (dashed line) and Facet Formation

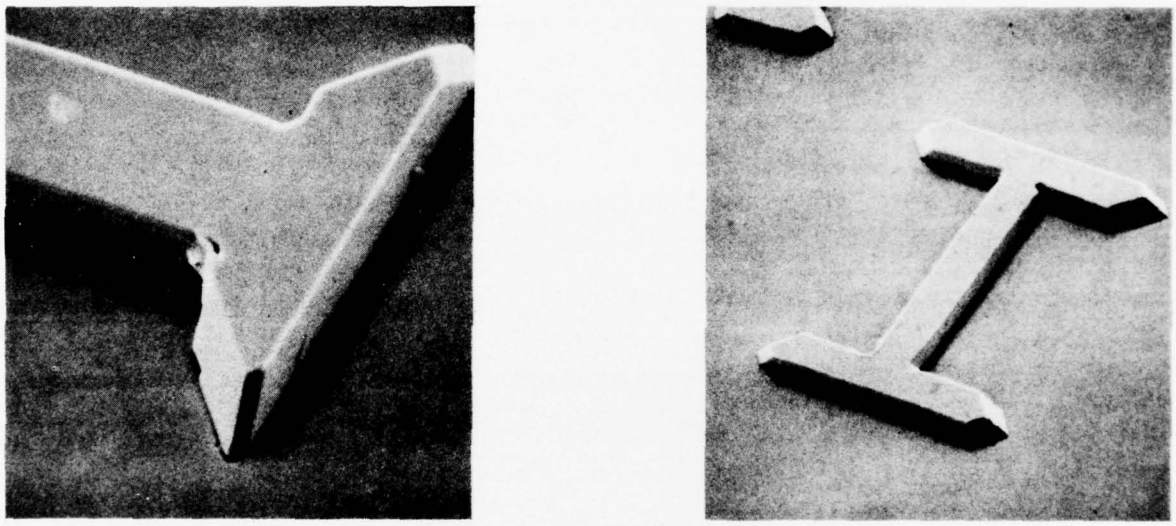

(a) (b)

Figure 8 SEM of I-Bar Mesas

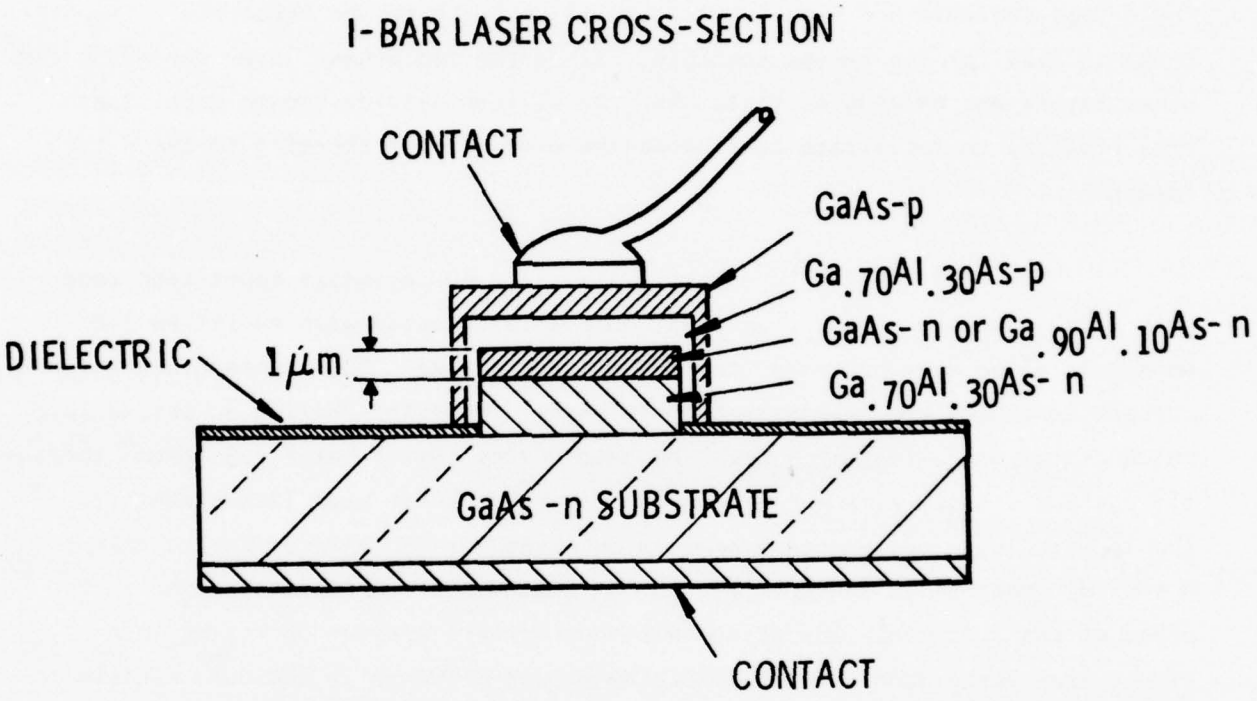

Figure 9 Cross Section of Layers in Double Heterojunction I-Bar Mesa Laser

I-bar lasers are grown in a stripe geometry that simplifies the fabrication process. Only p- and n-type contacts need to be affixed to the as-grown I-bars. The n-type contacts are made by electroplating Au-Sn to the substrate. Evaporated Cr-Au is used for the p-type contacts. Since the top p-GaAs layer surrounds the other layers and extends slightly over the silicon nitride growth mask, large area contacts to facilitate bonding can be used without shorting to the n-type layers.

The I-bar lasers have been tested at a 500 pulses/s repetition rate with a 200 ns pulse width. The light output is detected with an ITT FW 118 photomultiplier attached to a Spex 3/4 m spectrometer. Room temperature threshold current densities are typically 8 to 10 kA/cm^2 for lasers having an active layer thickness of approximately 1 μm. The best device tested has a 7.5 kA/cm^2 threshold current density with a 525 mA drive current. I-bar mesa lasers exhibit the longitudinal mode spectra commonly observed for Fabry-Perot cavity lasers. A typical spectrum is shown in Figure 10. Filaments are often observed in the plane of the junction, indicating that these lasers are not operating in a single transverse mode. I-bar lasers have been driven at a 40% duty cycle with a 1 MHz data rate with no additional provisions for heat sinking. External differential quantum efficiencies have been measured with a calibrated PIN photodiode,[19] and efficiencies as high as 15% have been observed.

5. Improved I-Bar Mesa Laser

The initial design of the I-bar mesa laser produced devices with 7.5 to 10 kA/cm^2 threshold current densities and 525 to 800 mA drive currents. To become acceptable for cw operation, these parameters must be reduced by at least a factor of 5, and a factor of 10 reduction will be necessary for them to become comparable to the better cleaved devices. Improvements in performance should be obtained from changes in the device geometries (dimensions) and fabrication process. A cross section of initial devices is shown in Figure 11. Using the as-grown narrow stripe geometry to obtain a buried heterostructure device

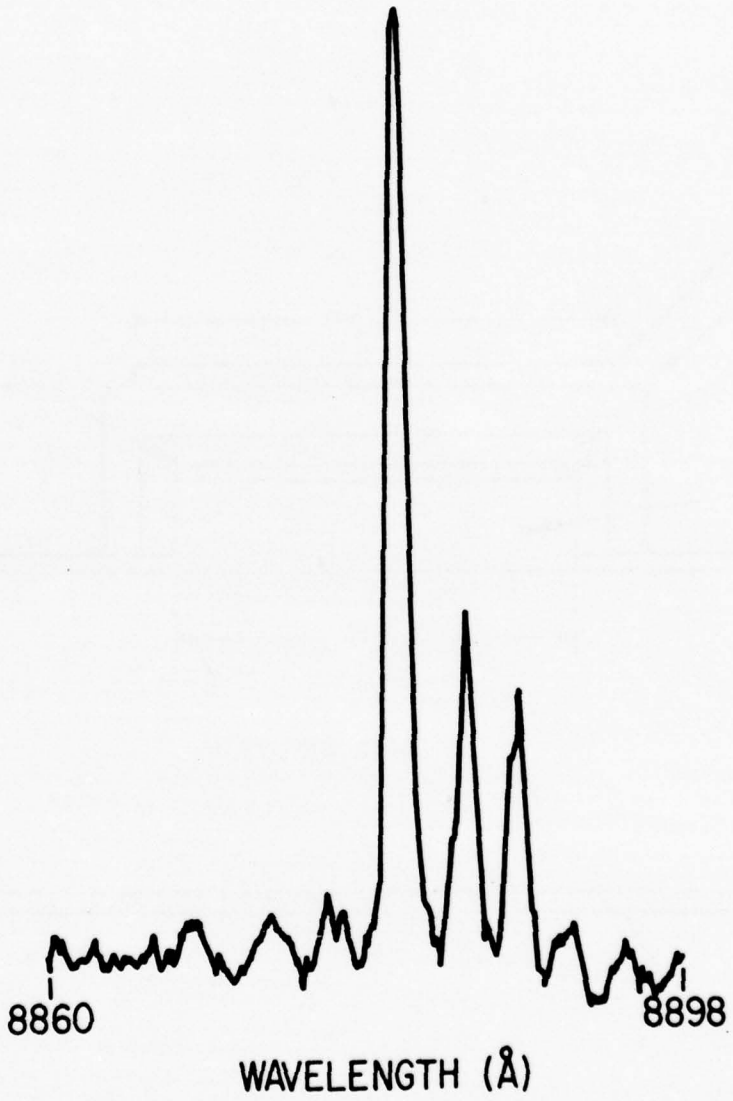

Figure 10 Optical Spectrum of I-Bar Mesa Laser

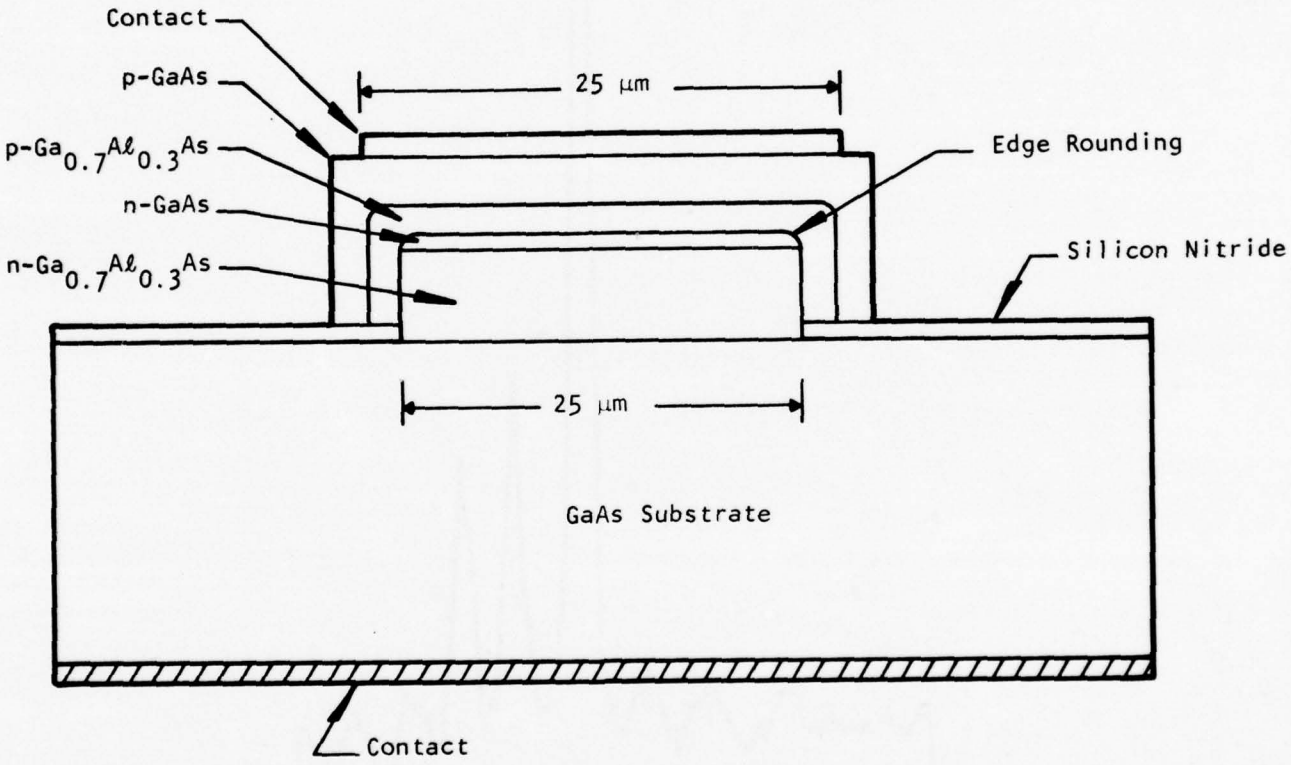

Figure 11 Cross Section of Initial I-Bar Devices

appears to have several practical drawbacks. First, to be truly effective as a buried heterostructure, the device should be very narrow (< 5 μm). We have been able to grow good I-bar devices with 25 μm wide stripes, but have not been able to control layer thicknesses for narrower stripe geometries. Although this may not be an insurmountable problem, it certainly increases the difficulties and decreases the yield. Second, the edges of the active layer usually are not a square facet, but are somewhat rounded or tapered. The nonuniformity in thickness can lead to filament-type behavior and inefficiencies in the laser. A stripe geometry over the more uniform central portion of the I-bar would be preferable. Third, because of the overlapping structure of the layers, there is a natural leakage current in the p-layers around the active layer and a subsequent loss in injection efficiency.

A cross section of a modified I-bar structure is shown in Figure 12. This structure combines the unique monolithic properties of the I-bar laser with present technologies involving stripe laser fabrication. The width of the I-bar is increased to 50 μm to improve layer control and decrease thicknesses. Stripe geometry lasers are fabricated on the I-bar using Zn diffusion and a silicon nitride mask to define the stripe injection region. The central location of the stripe is expected to minimize the edge effect and current leakage problems.

The new I-bar mesa structures have been grown, and the mesa features were found to be comparable to those of full surface discrete structures except for a minor loss in flatness in the top p-type GaAs contact layer. This could be corrected, if necessary, by minor modifications in the mask design. As anticipated, the change in geometry has altered the thicknesses of the epitaxial layers. Device fabrication procedures have been changed to incorporate stripe geometry fabrication technology. A new I-bar mesa laser after device processing is shown in Figure 13. The appropriate materials parameters for good lasers are presently being investigated. However, initial results are most encouraging for this new structure.

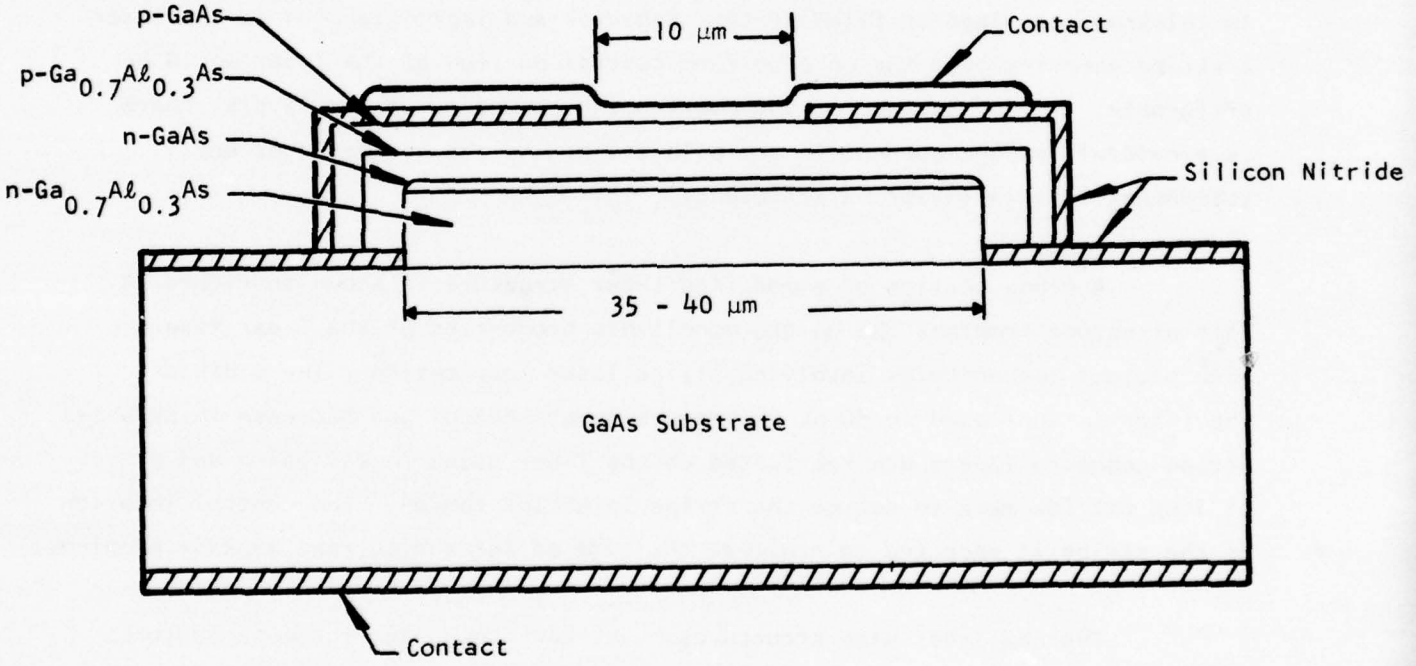

Figure 12 Cross Section of Modified I-Bar Laser

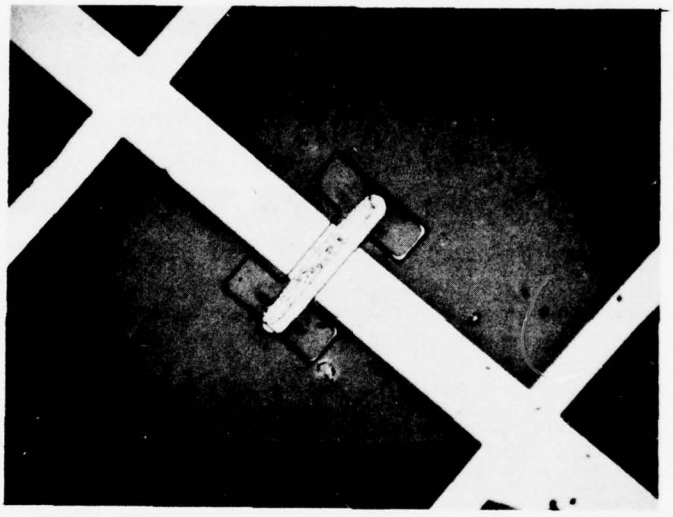

Figure 13 Modified I-Bar Mesa Laser after Zn Diffusion and Metal Contacting

SECTION III

GROWN WAVEGUIDES

The application of selective LPE to obtain an as-grown waveguide structure was spurred by the difficulties encountered in guiding light around bends. This capability is, of course, an absolute necessity to accomplish any light processing on a chip and thus achieve a truly integrated optical circuit. Early investigations using conventional dielectric striplines and rib waveguides were effective only for waveguides with a very large (> 1 cm) radius of curvature. Later work showed that closer confinement and guiding around bends could be obtained with very thin waveguides.[20-22] Waveguides grown by selective LPE have a larger change in the index of refraction in the lateral directions due to the embedded nature of the structure and thus should have improved confinement over the conventional planar structure. However, the increase in the index of refraction discontinuity will also increase the propagation losses of the guide.

Selective LPE waveguides have very different functional and structural requirements from the mesa laser. In addition to the general LPE limitations of narrow stripe geometries and naturally occurring facets mentioned previously, the waveguide must also (1) guide light in straight-line sections, (2) guide light around curves, (3) guide light from any one point on the chip to any other point, and (4) grow on {100} substrates. Straight-line waveguide sections can be readily grown in both the ⟨100⟩ and ⟨110⟩ directions and satisfies the straight-line sections in requirement (1). The combination of straight lines (1) and curves (2) can be designed to guide light between any two points (3).

The following subsections discuss the growth and properties of waveguides grown by selective LPE.

A. Materials Growth

The waveguides were grown by the same process described previously for the mesa lasers. The as-grown waveguides were usually three-layer structures with compositions of $Ga_{0.85}Al_{0.15}As$ - $Ga_{0.9}Al_{0.1}As$ - $Ga_{0.85}Al_{0.15}As$. Each of the

layers is about 2 μm thick. All of the layers were n-type, nominally undoped, with carrier concentrations in the low- to mid-$10^{16}/cm^3$ range. Several two-layer structures were also grown in which the top $Ga_{0.85}Al_{0.15}As$ layer was omitted.

Three different types of masks shown in Figure 14 and 15 were used for this study. Figure 14 shows two different waveguide patterns used only for waveguide studies. The radius of curvature (r_c) was set at values of 0, 0.254 mm (10 mils), 0.635 mm (25 mils), 1.27 mm (50 mils), 2.54 mm (100 mils), and 6.35 mm (250 mils). Stripe widths of both 10 μm and 25 μm were investigated.

Figure 15 shows a schematic of a more complex pattern used to form an integrated circuit with a laser. For waveguide test purposes, this pattern was cleaved along lines A and B. The two "legs" of the remaining structure had r_c values of 0 (9° angle of incidence) and 1.27 mm (50 mils). Only 25 μm stripe widths were used in this pattern. The unusual structural features of this pattern include the Y divider in the cleaved portion of the structure and the "funnel" at the top of the guide for collecting light from the laser.

The faceting in the bend for waveguides with different radii of curvature is shown in Figure 16. For $r_c \leq 0.254$ mm (10 mils), there is substantial overgrowth and faceting in the bend. For $r_c \geq 0.635$ mm (25 mils), however, smooth nonfaceted outer surfaces can be obtained. Figure 17 contains SEM photographs of sets of four 10 μm wide, three-layer waveguides with $r_c = 1.27$ mm (50 mils) and 2.54 mm (100 mils) and a cross section of a three-layer waveguide. Complex patterns containing straight lines, curves, and Y dividers, such as shown in Figure 18 can be readily grown. This structure will be discussed further in the section on integrated structures.

B. Waveguide Characteristics

Light guiding has been observed for all waveguide structures including $r_c = 0$ (9° angle of incidence) with 2 to 3 μm thick waveguide layers. Figure 19

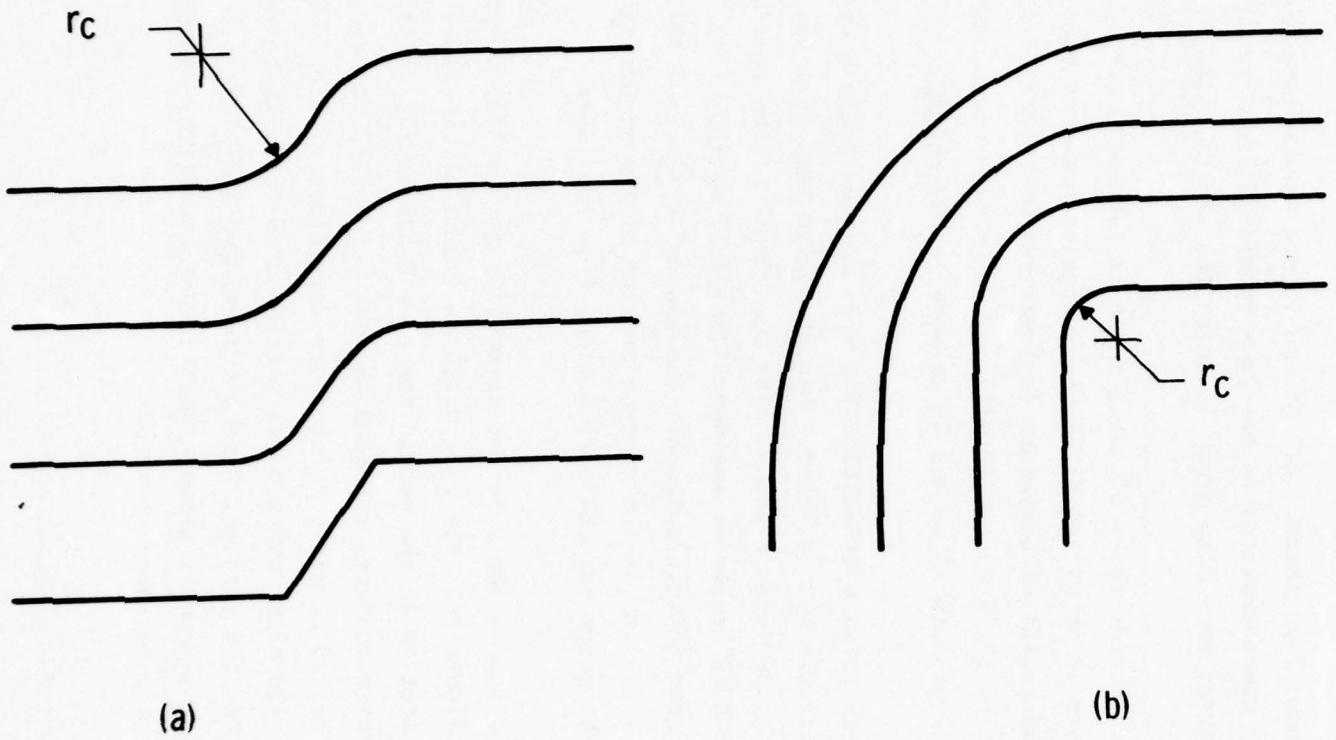

Figure 14 Schematic Drawing of Various Bend Configurations for Waveguides

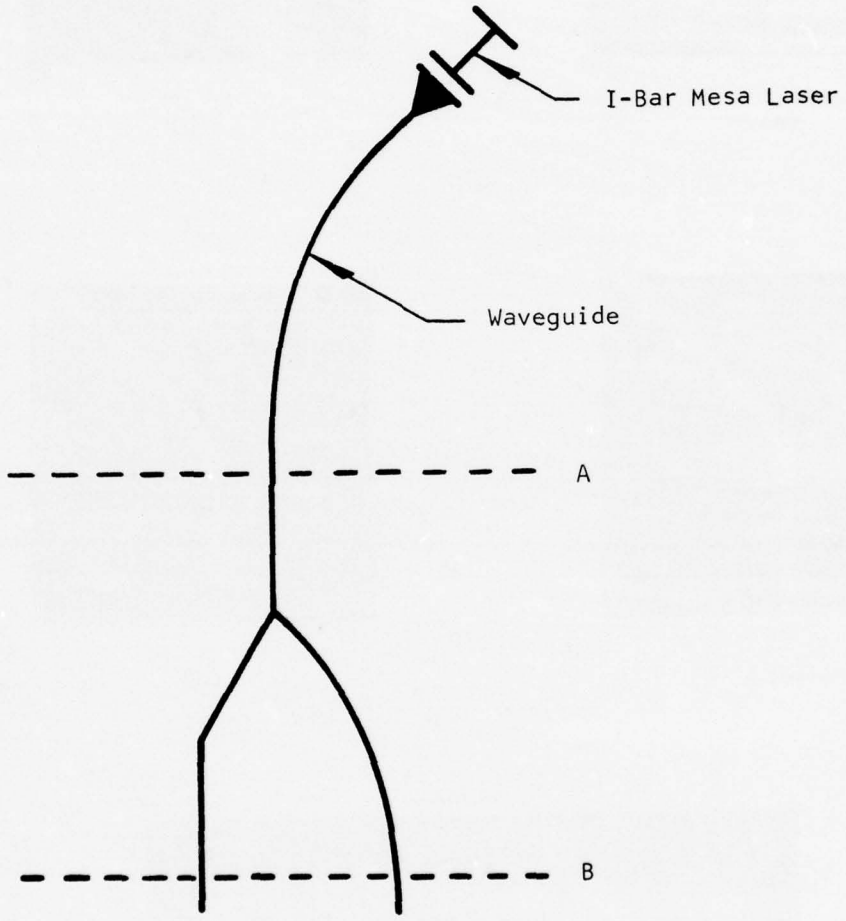

Figure 15 Schematic of Waveguide Pattern with Complex Geometries

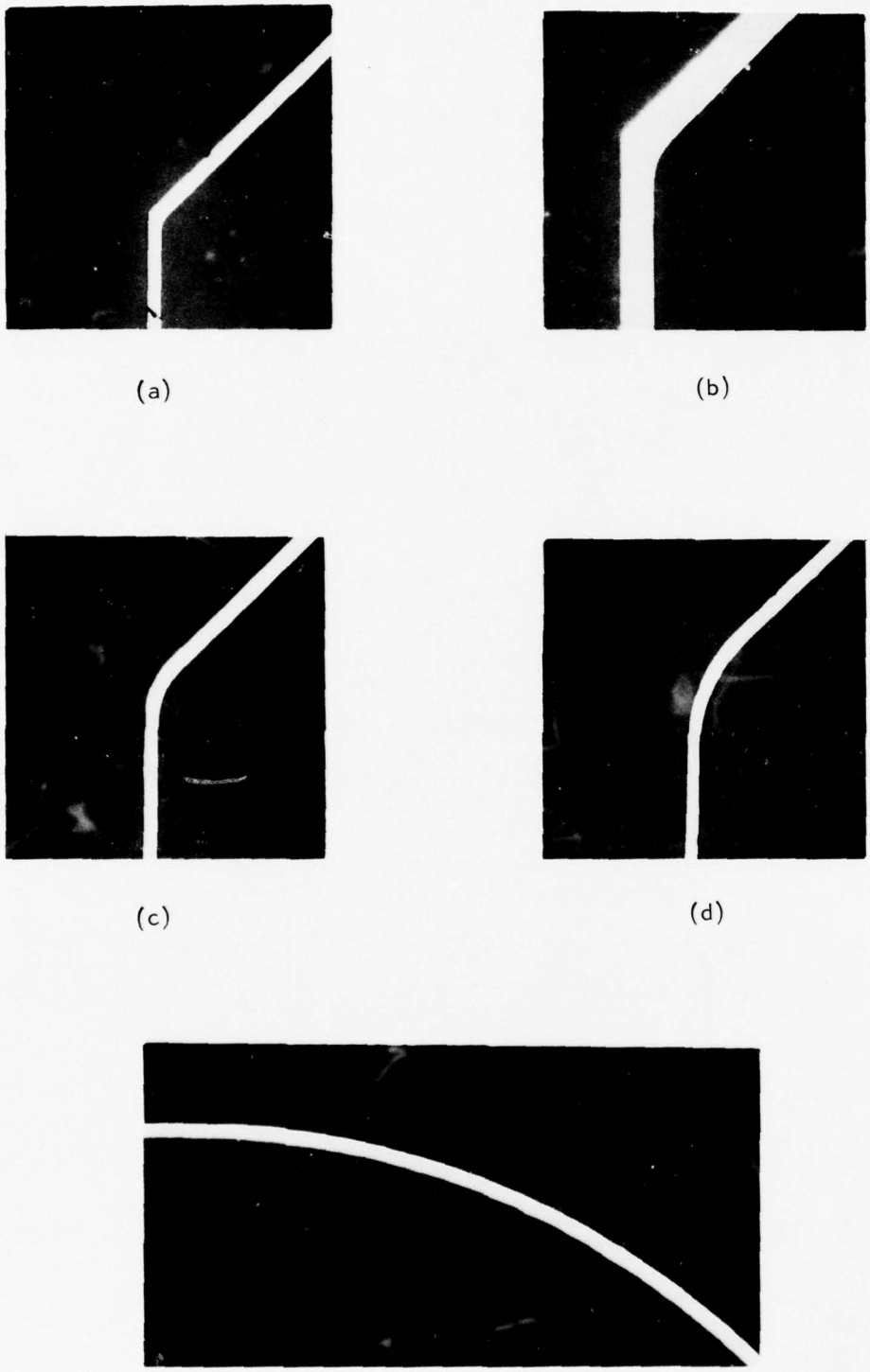

Figure 16 As-Grown Waveguides with Radii of Curvature (a) 0, (b) 0.254 mm (10 mils), (c) 0.635 mm (25 mils), (d) 1.27 mm (50 mils, and (e) 6.35 mm (250 mils)

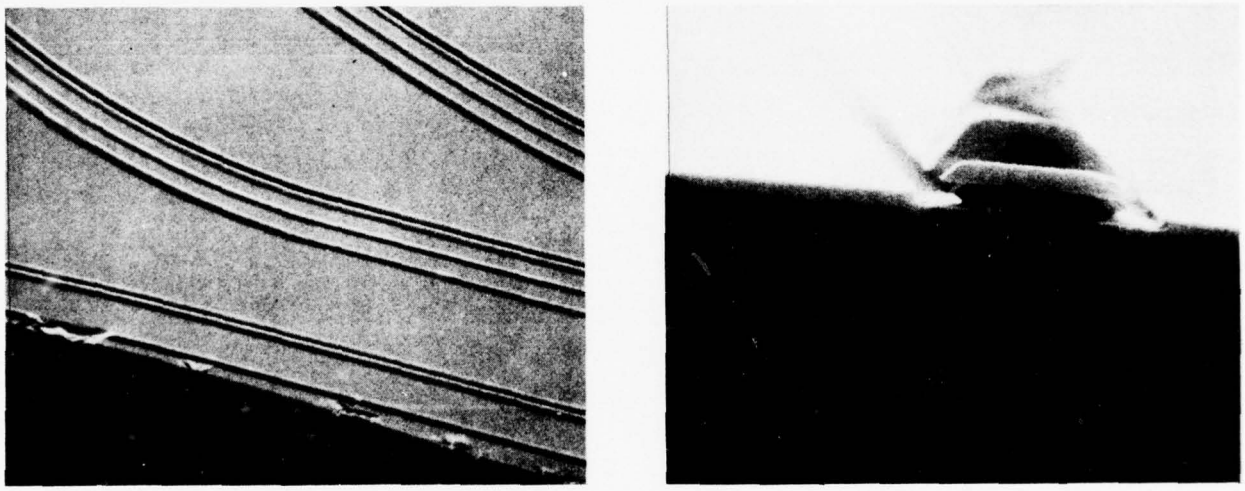

Figure 17 SEM of Selective LPE Waveguides Showing Growth Around a Bend and a Cross Section of a Three-Layer Waveguide

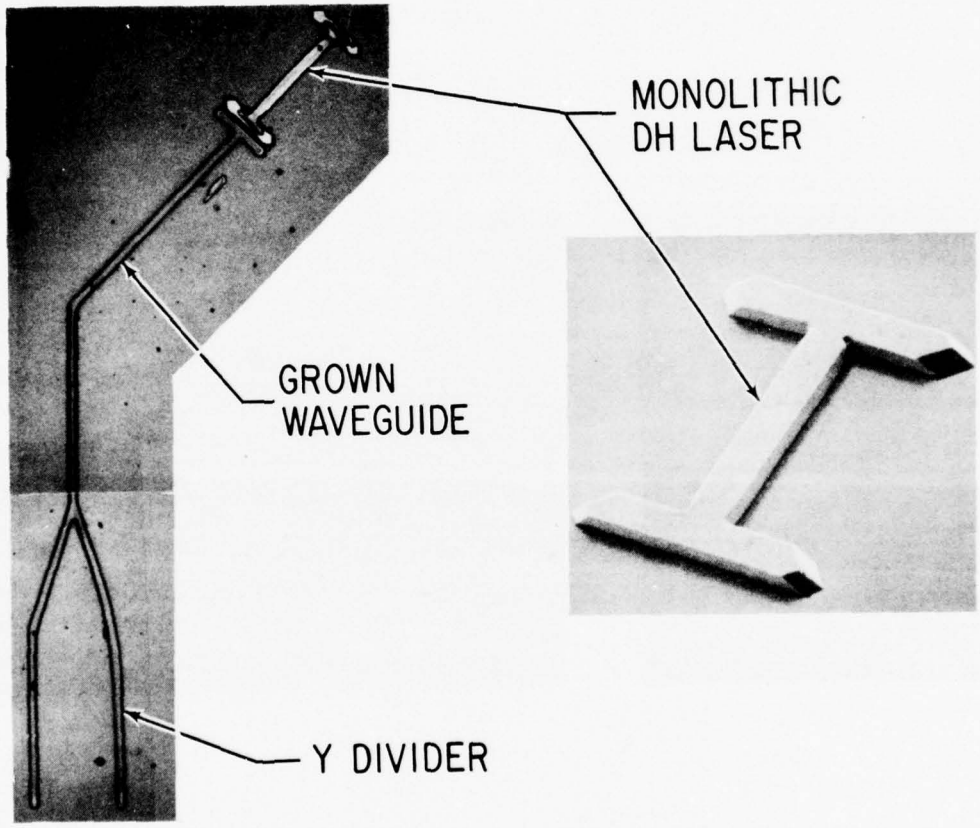

Figure 18 Complex Grown Waveguide Structure Including Straight Lines, Curves, and Y Dividers

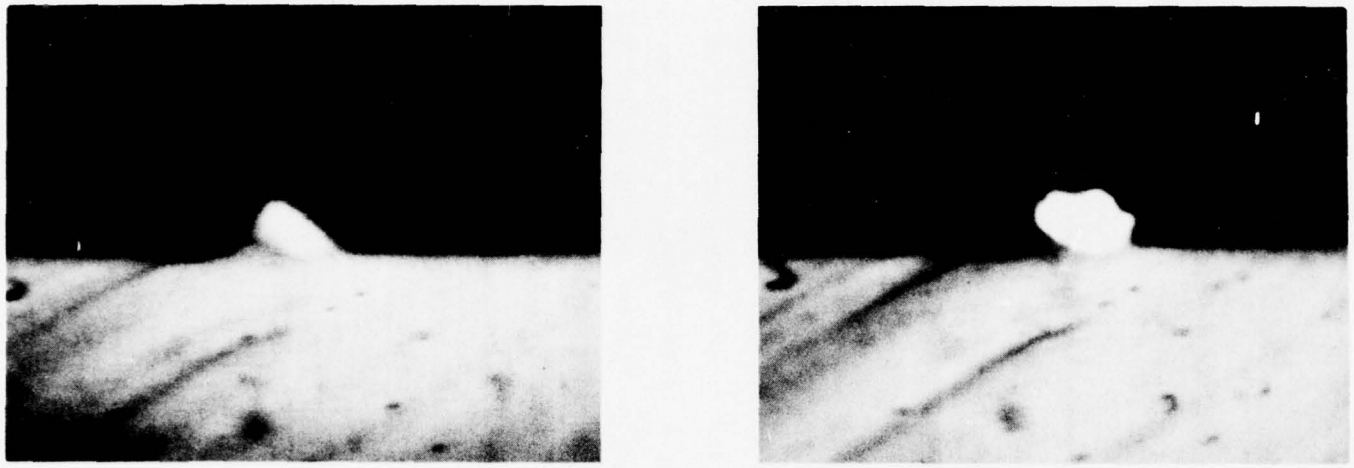

(a) (b)

Figure 19 TV Pictures of (a) an As-Grown Waveguide and (b) Light Guiding in the Waveguide

shows TV pictures taken with a vidicon camera of (a) an as-grown waveguide above the substrate, and (b) light guiding in the waveguide. As anticipated from the larger index of refraction discontinuity, the losses in straight-line sections are higher for the as-grown waveguides (9 to 18 dB/cm) than for the LPE (Ga,Aℓ)As planar rib waveguides (5 to 7 dB/cm). The loss values are also enhanced by materials inhomogeneities and defects in the long guide sections required to make these measurements. Improvements in the materials growth process would be expected to lessen the contribution from this area.

Due to the uncertainty in the loss measurements, it has not been possible to define absolute loss values associated with different radii of curvature. However, some relative values and trends have been obtained. Table II indicates the typical values obtained for a three-layer, as-grown waveguide. In this sample, ∞ is a straight-line guide adjacent to the curved guides and used as standard. As expected, the trend is toward increasing loss with decreasing radius of curvature. Rapid degradation occurs for $r_c < 1.27$ mm (50 mils) and places a lower limit on the range of interest for practical circuit design. Similar behavior was observed for the waveguide section of Figure 15 where the relative outputs of the two "legs" was $r_c(1.27\ \text{mm})/r_c(0) \sim 12$.

The as-grown waveguides have proved to be efficient in guiding light around bends. The straight-line losses, however, are too high at this time to be efficient in all sections of a waveguide circuit. Improvements in materials technology may lower the loss values to a more acceptable level, but with the present technology a hybrid circuit with as-grown guides around bends and low-loss planar rib guides in straight sections and for active devices appears to be the best compromise.

Table II

Signal Output for Three-Layer Waveguides

R_c (Mils)	R_c (mm)	Signal Out (mV)	Normalized Signal (mV)
∞*	∞	6	1
100	2.540	4.2	0.7
50	1.270	3.8	0.63
25	0.635	0.6	0.1
0	0	0	0

* Straight-Line Waveguide

SECTION IV

COUPLED I-BAR DOUBLE HETEROJUNCTION MESA LASERS AND WAVEGUIDES

Selective LPE mesa lasers and waveguides can be combined in a two-step process to produce an integrated circuit. This has been accomplished as shown in Figure 20 and marks a major milestone in the progress of this program. The following subsections will discuss the materials technology, fabrication, and test results for this device.

A. Materials Growth and Fabrication

The integrated I-bar mesa laser structure is produced in a two-step selective LPE process. The selective LPE procedures are the same as those described in the previous two sections. The overall design of the device as shown in Figure 21 consists of two separate masks, one for the waveguide structure and one for the mesa laser structure. In the first growth step the three-layer waveguide structure is grown in the waveguide pattern only. The mesa laser area in this step is covered by the silicon nitride mask. After the first growth step, the silicon nitride mask is stripped and the entire substrate, including the grown waveguide, is covered with fresh silicon nitride. The laser pattern is then opened in the mask and the DH I-bar mesa laser is grown in the second LPE growth step. Figure 22 shows the position of the mesa laser relative to the waveguide after the second growth step. The laser in this circuit is end-fired into the waveguide. Differences in the reflectivity in Figure 22 are due to the dielectric coating over the waveguide in this step. Ohmic contact to the back of the unthinned substrate is made by alloying electroplated Ni-Au at 300°C. The p-type contact on the top of the mesa is made by evaporating Cr-Au. A wide bonding pad at the side of the mesa permits off-mesa bonding. The final test device is cleaved along line A of Figure 21 to give single-channel light output. A finished device mounted on a TO-46 header is shown in Figure 23.

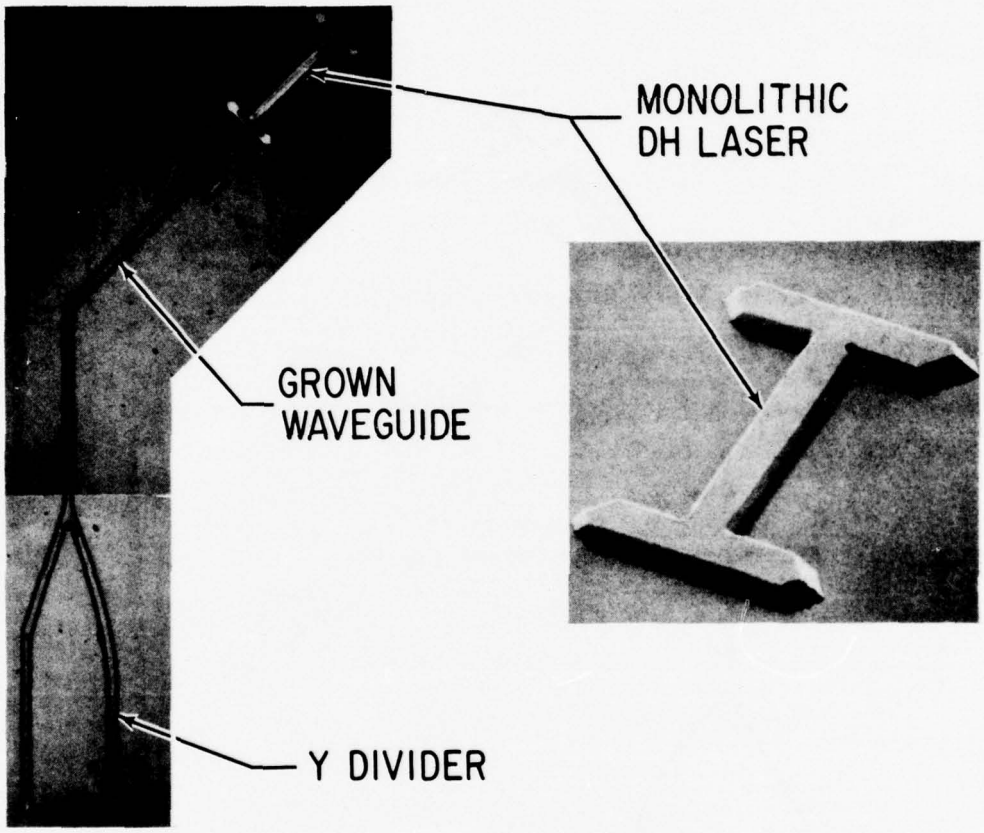

Figure 20 Selective LPE I-Bar Laser-Waveguide Integrated Circuit

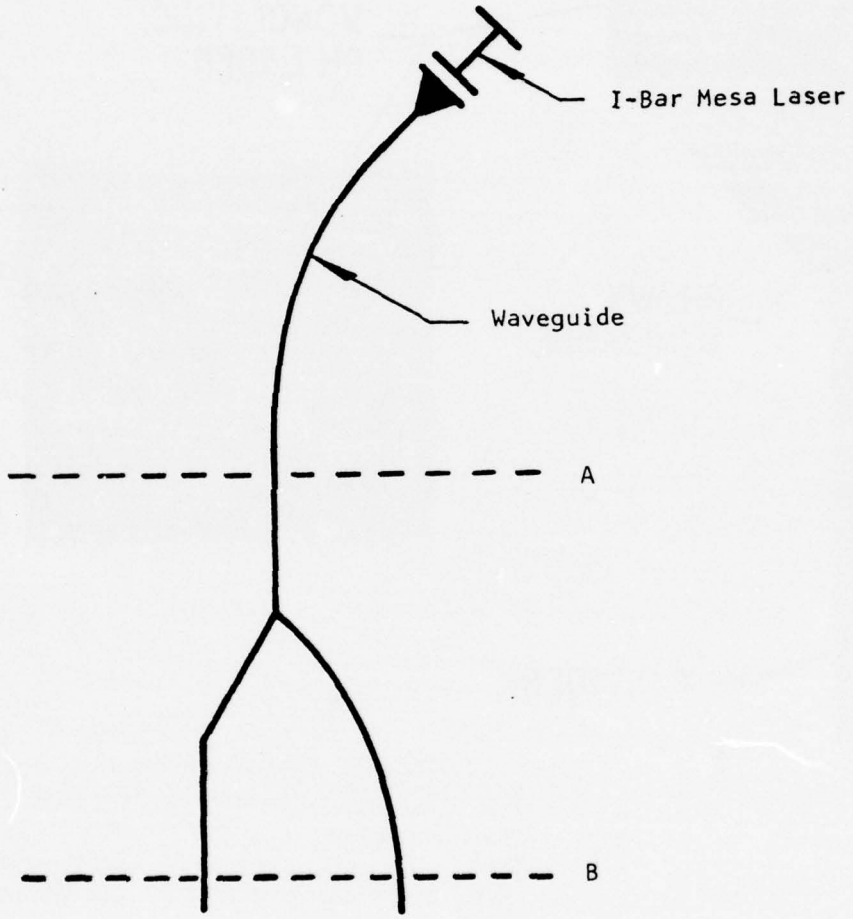

Figure 21 Integrated I-Bar Mesa Laser-Waveguide Structure

Figure 22 Photomicrograph (~ 20X) Showing the As-Grown Mesa Laser-Waveguide with a 0.254 mm (10 Mils) Radius Prior to Contacting. Differences in reflectivity are due to the dielectric coating over the waveguide.

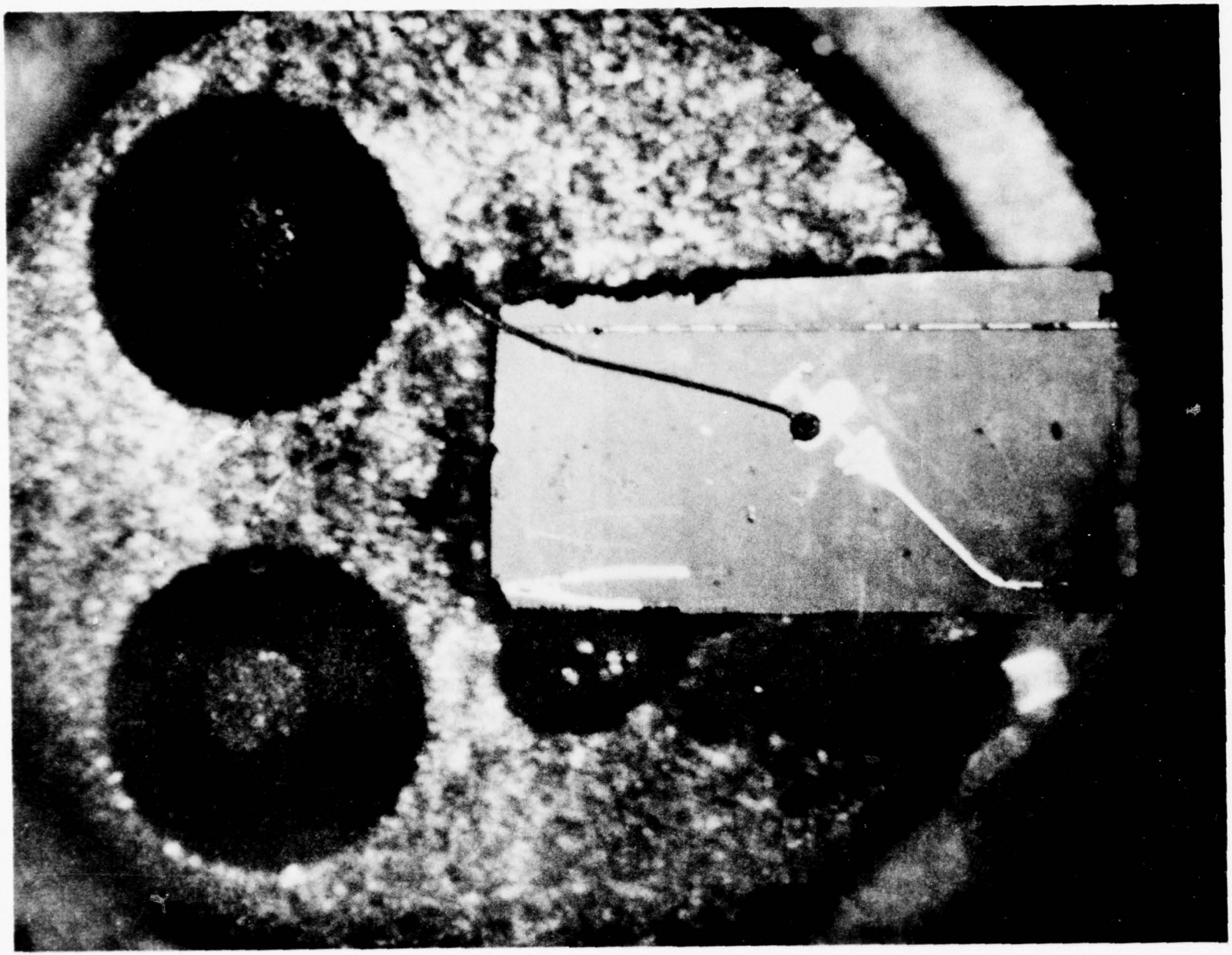

Figure 23 Photomicrograph (~ 10X) of the First Integrated Optical Circuit with an I-Bar Mesa and Channel Waveguide with Bend Mounted on a TO-46 Header

B. Device Performance

I-bar mesa laser-waveguides have been successfully fabricated and tested. The I-bars had been grown prior to the materials improvements previously mentioned. These devices had active regions of 1.5 μm and correspondingly high thresholds of 40 kA/cm^2. The as-grown waveguides are three-layer structures with nominal compositions of $Ga_{0.8}Al_{0.2}As$ - $Ga_{0.85}Al_{0.15}As$ - $Ga_{0.8}Al_{0.2}As$ with the central layer about 4.0 μm thick. Laser radiation from the I-bar was end-fired-coupled to the curved waveguide. Its radius of curvature was a severe 0.254 mm (10 mils). Measurements of the light transmitted through the waveguide and from the laser showed a transmission of about 35% of the laser output. The output was narrowband, suggesting that a selection of laser modes is taking place. The transmission figure was based on the power in the narrowband laser output, not on the total emission power spectrum of the laser. This unexpected selectivity is not understood at this time.

The successful testing of this device is a major accomplishment in this program. Although this structure has limitations which have become obvious in the growth, fabrication, and testing, it is a significant first step toward practical integration and supplies invaluable information in the design of the next-generation device.

SECTION V

ETCHED MESA DOUBLE HETEROJUNCTION LASERS AND WAVEGUIDES

One of the key problems in the development of integrated optical circuits is that of efficiently coupling light from a monolithic laser source to a waveguide circuit. Three coupling schemes have previously been reported: (1) end-fire coupling,[23,24] (2) taper coupling,[25,26] and (3) phase-matched coupling.[27,28] Devices using end-fire coupling have passive waveguides coplanar with the laser cavity. An alternate approach utilizes an intracavity taper to couple light from the laser to an underlying waveguide. A disadvantage of these coupling schemes is that they require the utmost control of the growth conditions[24,26] or a two-stage growth procedure.[23] A less complicated structure, from a fabrication point of view, has been reported by Suematsu, et al.[28,29] In these lasers the coupling between the laser cavity and an external passive waveguide is analogous to that of a directional coupler. To obtain efficient coupling, the propagation constants of the laser cavity and the passive waveguide must be closely matched. This imposes severe limitations on the dimensions and compositions of the layers. In this section we describe a device similar to the structure reported by Suematsu, et al.,[28,29] consisting of a monolithic laser on an underlying passive waveguide. The coupling mechanism differs, however, in that the modes of the waveguide are excited directly by the evanescent fields of radiation in the laser cavity without phase matching.

The following subsections discuss the device structure, the growth and fabrication, and test results for the etched mesa laser-waveguide structures.

A. Device Structure

The schematic in Figure 24 shows the structure for the laser-waveguide five-layer device with typical layer compositions and thicknesses. Starting from the substrate, the LPE layers are n-type $Ga_{0.7}Al_{0.3}As$ (3 μm), n-type $Ga_{0.85}Al_{0.15}As$ (5 μm), n-type GaAs active layer (0.5 μm), p-type $Ga_{0.7}Al_{0.3}As$ (1.5 μm), and p-type GaAs (1 μm) for contacting. The six-layer devices have

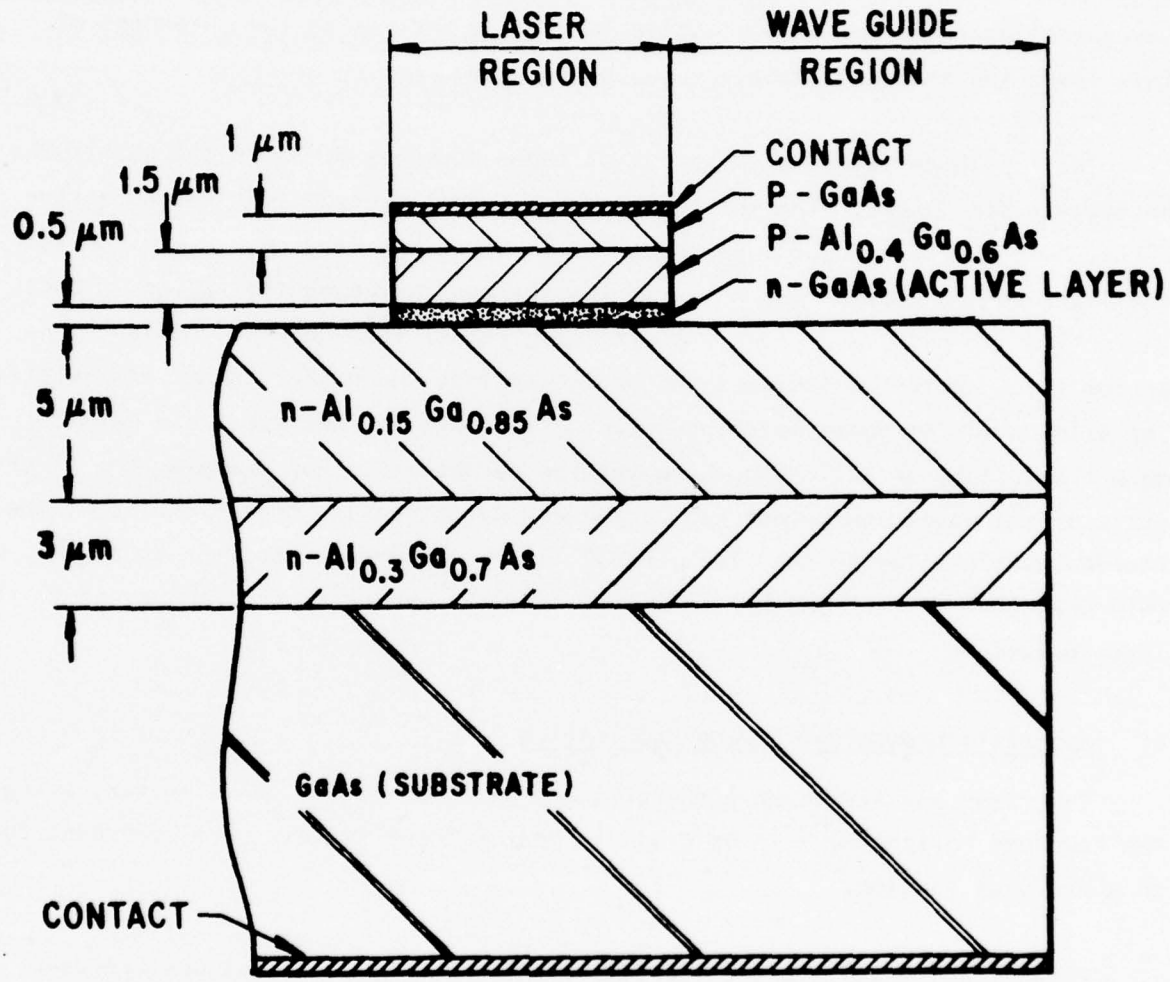

Figure 24 Schematic of the Etched Mesa Laser-Waveguide Five-Layer Structure

an additional thin n-type $Ga_{0.7}Al_{0.3}As$ (0.5 μm) layer between the n-$Ga_{0.85}Al_{0.15}As$ waveguide layer and the n-GaAs active layer. By increasing the thickness of this layer the amount of coupling can be reduced.

The top three layers are typical of those commonly found in (Al,Ga)As/GaAs heterojunction lasers. The fourth layer has a dual function; it serves as the n-type heterobarrier as well as being the "external" waveguide. Radiation in the laser region excites the modes of the surrounding waveguide region. Hence, the active and passive regions are strongly, rather than weakly, coupled. The bottom layer optically isolates the waveguide from the higher index GaAs substrate. The elimination of phase matching between the laser and the substrate permits more flexibility in tailoring the waveguide parameters. For example, the divergence of the waveguide output can be reduced by increasing the thickness of the fourth layer similar to the "leaky wave" lasers reported by Scifres et al.[30] This structure has the further advantage that the waveguide is transparent to the laser emission.

B. Materials Growth and Device Fabrication

The five- and six-layer structures are grown by liquid phase epitaxy using the standard horizontal sliding graphite boat. These systems have been described in a previous section.

Following crystal growth, standard photolithographic techniques are used to define a silicon nitride mask consisting of rectangles 300 μm x 200 μm. The crystal is then chemically etched in two steps. First, a calibrated $NaOH:H_2O_2$ etch[31] is used to remove the top three layers and etch into the fourth layer. This is followed by a 30 minute etch in the Superoxol solution described by Logan and Reinhart.[32] Since the Superoxol solution etches GaAs faster than (Al,Ga)As, this second etching step helps to "square up" the ends of the laser cavity as illustrated by the photograph in Figure 25. We find that the Superoxol etch is an important fabrication step that can in some instances be the difference

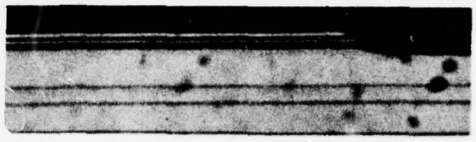

Figure 25 Cross Section of an Etched Mesa after the Second Preferential Etch to "Square Up" the Ends of the Laser Cavity

between a device that will lase and one that will not. The etching procedure can be used to control the degree of coupling. Etching partially into the waveguide results in increased reflectivity and a reduction in the amount of light coupled into the waveguide. Contact to the top of the etched mesa is made by selectively electroplating Au-Ni. An alloyed Au-Sn contact is made to the back of the substrate. For testing, the devices are soldered on the edge of TO-46 headers. The lasers are driven with 200 ns current pulses at a repetition rate of 100 Hz.

C. Device Testing and Results

Figure 26 is a photograph of the near field emission from an etched laser-waveguide device above threshold. The photograph was taken with an infrared microscope focused on the end of the waveguide and thus misrepresents the relative amount of light emerging from the waveguide compared to that from the laser. It does, however, clearly illustrate light coupling from the laser to the waveguide. The coupling efficiency of these devices is measured with a calibrated PIN photodiode in three steps. First, the total output from the laser and waveguide is measured for increasing drive current. Then the power in the waveguide is determined by blocking off light from the laser with a knife edge positioned between the laser and the end of the waveguide. Finally, the background light is measured with the knife edge in position and the end of the waveguide masked with a thick layer of black wax.

Figures 27 and 28 are representative of the data obtained by this procedure. These data were taken on five-layer and six-layer devices, respectively. The dashed curve and solid curve show the power in the laser and the waveguide, respectively. For the six-layer devices the average coupling efficiency (i.e., the percentage of the laser power coupled into the waveguide) was approximately 10%. The average laser threshold current density was 2.6 kA/cm^2. This is approximately 15% higher than cleaved discrete lasers fabricated from the same crystal. The increased laser threshold is due primarily to the additional loss of light into the waveguide and can be compensated by fabricating mirrors on the

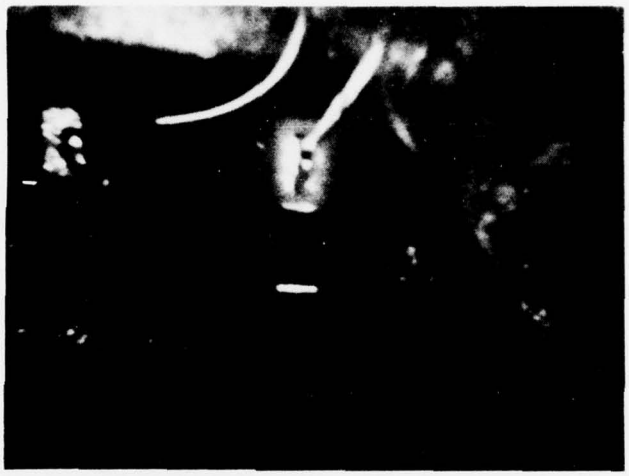

Figure 26 Near Field Emission from an Etched Laser-Waveguide Device above Threshold. The mesa laser is shown as the bright area under the contact. The bright spot in the foreground is the output from the waveguide layer at the cleaved face.

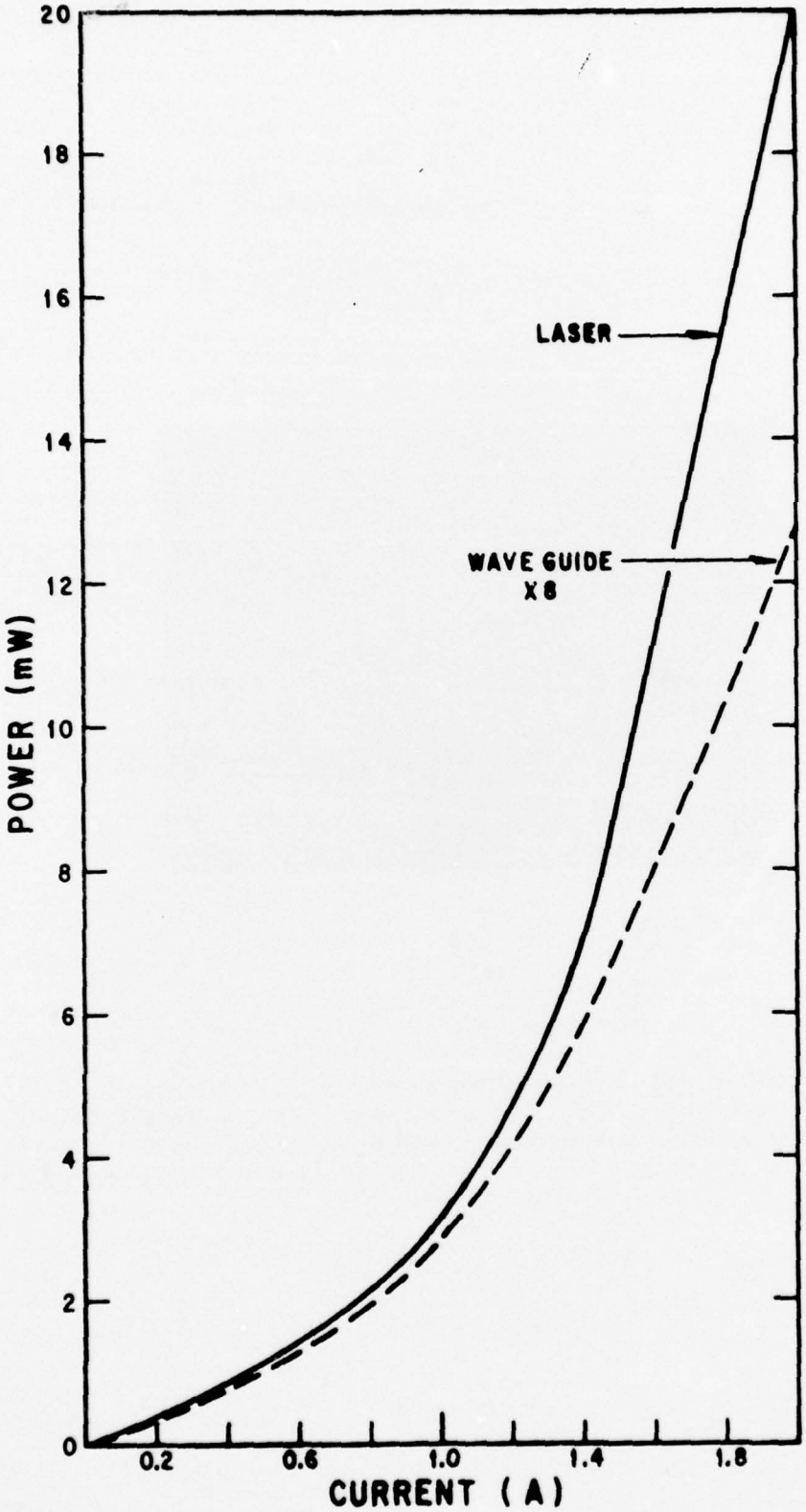

Figure 27 Power Output for the Laser and for the Waveguide in a Five-Layer Structure

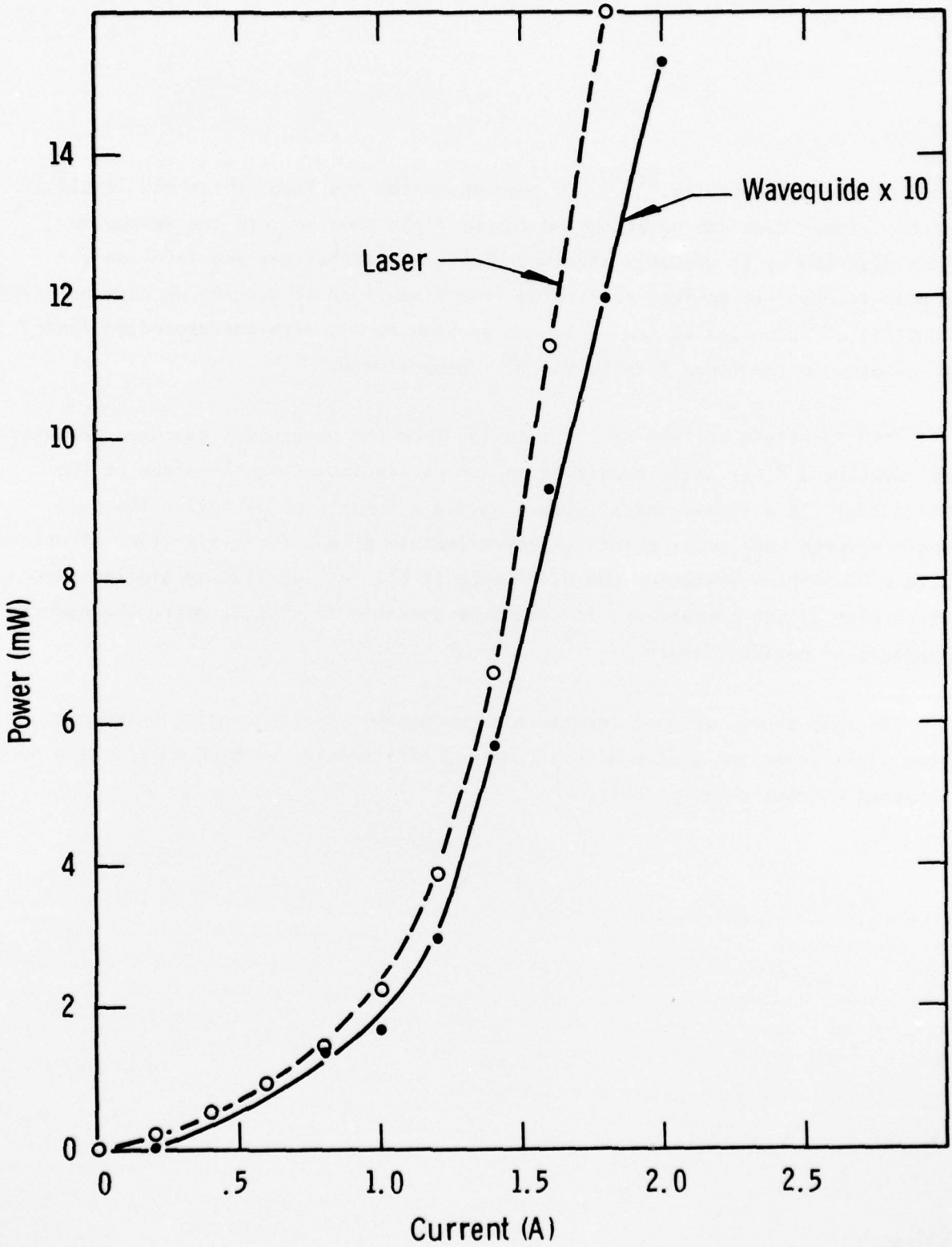

Figure 28 Power Output Measured for the Laser and for the Waveguide in a Six-Layer Structure

ends of the laser cavity.[28,29] In some instances the laser threshold is significantly higher than can be accounted for by light coupled into the waveguide. This discrepancy is probably attributable to unsatisfactory end faces on the etched lasers. In devices fabricated from five-layer structures we have observed coupling efficiencies as low as 3% and as high as 25% with corresponding laser thresholds in the range 3 to 10 kA/cm^2, respectively.

The far-field pattern of the emission from the waveguides has been measured by rotating a fiber optic bundle in an arc perpendicular to the plane of the waveguide. In a five-layer structure having a 5 μm-thick waveguide the full angle between half power points is approximately 5° and for a six-layer structure with a 4 μm-thick waveguide the divergence is 6°. By fabricating similar structures with stripe geometries, it should be possible to closely match the numerical aperture of optical fibers.

In this study, we have demonstrated evanescent field coupling between a monolithic laser and a waveguide. Coupling efficiencies as high as 25% have been obtained without phase matching.

SECTION VI

CONTACTING INVESTIGATIONS

Work on reducing contact resistance on both I-bar and full-surface discrete lasers has continued. In order to achieve cw operation, series contact resistance (i.e., the diode series resistance) should be less than 1 Ω at the threshold current. Lower resistances, however, will increase the total power conversion efficiency. The major contribution to this series resistance arises from the metal-semiconductor-interface resistance. The lowest series resistance observed on our discrete lasers is 0.2 Ω; on the mesas, 7.0 Ω. These values correspond to the same specific contact resistances of 2×10^{-4} Ω-cm^2 due to the differences in contact area. The improvement in discretes is due primarily to the introduction of a premetallization zinc diffusion into the surface p-type GaAs layer. Hole concentrations of 10^{20}/cc are achieved. In addition, Au-Zn or Ag-In-Zn followed by Ti-Au, Cr-Au, or Ni-Au metallization by evaporation or electroplating completes the contact. The higher resistance observed with mesa lasers is believed to be due to difficulties in cleaning the surface for the striped contact.

SECTION VII

SUMMARY AND RECOMMENDATIONS

As a result of the innovative materials and device developments on the present phase of this program, the first truly monolithic double heterojunction GaAs/GaAℓAs laser has been made. This laser operating pulsed at 300 K was integrated with grown GaAℓAs waveguides to form the first integrated optical circuit. Various design parameters for waveguides with bends and Y's were also established, as were present limitations on this monolithic laser performance.

It is clear that improvement of the mesa laser performance for cw operation at 300 K is the next step in its evolution. As suggested in detail, the basic structure of the I-bar can be modified to give better control of the active layer thickness, which affects the lasing threshold current density, and to limit the injection region with a subsequent decrease in drive current. These material improvements will then be complemented by lower resistance contacts and heat sinking technique to give reliable, long-life lasers for sources on integrated optical circuits.

REFERENCES

1. F. A. Blum, D. W. Bellavance, J. C. Campbell, and K. L. Lawley, "Monolithic Laser," Annual Interim Report, Contract No. N00014-73-C-0288, July 1975.

2. M. B. Panish, J. Appl. Phys. 44, 2667 (1973).

3. K. K. Shih and G. D. Pettit, J. Electron. Mat. 3, 391 (1974).

4. C. J. Hwang and J. C. Dyment, J. Appl. Phys. 44, 3240 (1973).

5. F. E. Rosztoczy and K. B. Wolfstirn, J. Appl. Phys. 42, 426 (1971).

6. A. J. Springthorpe, F. D. King, and A. Becke, J. Electron. Mat. 4, 101 (1975).

7. D. L. Rode, R. L. Brown, and M. A. Afromowitz, J. Cryst. Growth 30, 299 (1975).

8. J. P. Chane, L. Hollan, and C. Schiller, J. Cryst. Growth 13/14, 325 (1972).

9. S. Iida and K. Ito, J. Cryst. Growth 13/14, 336 (1972).

10. D. W. Shaw, R. W. Conrad, E. W. Mehal, and O. W. Wilson, Proceedings of the 1966 Symposium on GaAs, p. 10.

11. D. W. Shaw, J. Electrochem. Soc. 113, 904 (1966).

12. D. W. Shaw, J. Electrochem. Soc. 115, 777 (1968).

13. T. Mikawa, O. Wada, and H. Takanashi, Japan J. Appl. Phys. 11, 1756 (1972).

14. T. Kawakami and K. Sugiyama, Japan J. Appl. Phys. 12, 1808 (1973).

15. I. Samid, C. P. Lee, A. Gover, and A. Yariv, Appl. Phys. Lett. 27, 405 (1975).

16. D. W. Bellavance, unpublished results.

17. F. A. Blum, K. L. Lawley, W. C. Scott, and W. C. Holton, Appl. Phys. Lett. 24, 430 (1974).

18. F. A. Blum, K. L. Lawley, F. H. Doerbeck, and W. C. Holton, Appl. Phys. Lett. 25, 620 (1974).

19. E. Pinkas, B. I. Miller, I. Hayashi, and P. W. Foy, J. Appl. Phys. 43, 2827 (1972).

20. J. K. Butler, C. S. Wang, and J. C. Campbell, J. Appl. Phys. 47, 4033 (1976).

REFERENCES

(Continued)

21. K. L. Lawley and J. C. Campbell, "(Aℓ,Ga)As Devices for Waveguide Circuits," Technical Report No. 2, Contract No. N00014-75-C-0501, July 1976.

22. J. C. Campbell and D. W. Bellavance, "Bends and Curves in Optical Stripline Waveguides," Presented at the Device Research Conference, June 1976; Abstract IIA-3 (to be published).

23. C. E. Hurwitz, J. A. Rossi, J. J. Hsieh, and C. M. Wolfe, Appl. Phys. Lett. 27, 241 (1975).

24. F. K. Reinhart and R. A. Logan, Appl. Phys. Lett. 25, 622 (1974).

25. J. L. Merz, R. A. Logan, W. Wiegmann, and A. C. Gossard, Appl. Phys. Lett. 26, 337 (1975).

26. F. K. Reinhart and R. A. Logan, Appl. Phys. Lett. 26, 516 (1975).

27. R. K. Watts, J. Appl. Phys. 44, 5635 (1973).

28. Y. Suematsu, M. Yamada, and K. Hayashi, Proc. IEEE (Lett.) 63, 208 (1975).

29. Y. Suematsu, M. Yamada, and K. Hayashi, IEEE J. Quantum Electron. QE-11, 457 (1975).

30. D. R. Scifres, W. Streifer, and R. D. Burnham, Appl. Phys. Lett. 29, 23 (1976).

31. T. Kobayashi and K. Sugiyama, Jap. J. Appl. Phys. 12, 619 (1973).

32. R. A. Logan and F. K. Reinhart, J. Appl. Phys. 44, 4172 (1973).

APPENDIX

CONFERENCE PRESENTATIONS AND PUBLICATIONS

APPENDIX

CONFERENCE PRESENTATIONS AND PUBLICATIONS

Presentations

1. D. W. Bellavance and J. C. Campbell, "Mesa Lasers with Room Temperature Operation Grown by Selective Liquid Phase Epitaxy," Topical Meeting on Integrated Optics, Salt Lake City, Utah (January 1976).

2. J. C. Campbell and D. W. Bellavance, "Bends and Curves in Optical Stripline Waveguides," 1976 Device Research Conference, Salt Lake City, Utah (June 1976).

3. D. W. Bellavance and J. C. Campbell, "Selective Liquid Phase Epitaxy for Integrated Optical Circuits," 6th International Symposium North American Conference on GaAs and Related Compounds, St. Louis, Missouri (September 1976).

4. D. W. Bellavance and J. C. Campbell, "$Ga_{1-x}Al_xAs$ Waveguides Grown by Selective Liquid Phase Epitaxy," 150th Meeting of the Electrochemical Society, Las Vegas, Nevada (October 1976).

Publications

*1. D. W. Bellavance and J. C. Campbell, "Room-Temperature Mesa Lasers Grown by Selective Liquid Phase Epitaxy," Appl. Phys. Lett. 29, 162 (1976).

2. D. W. Bellavance and J. C. Campbell, "Selective Liquid Phase Epitaxy for Integrated Optical Circuits," to be published in the Proceedings of the North American Conference on GaAs and Related Compounds.

3. J. C. Campbell and D. W. Bellavance, "Monolithic Laser/Waveguide Coupling by Evanescent Fields," to be published in the IEEE J. Quantum Electron.

* Reprint attached

Room-temperature mesa lasers grown by selective liquid phase epitaxy*

D. W. Bellavance and J. C. Campbell

Texas Instruments Incorporated, Central Research Laboratories, Dallas, Texas 75222
(Received 30 April 1976)

A new monolithic mesa laser structure grown by liquid phase epitaxy through openings in a silicon nitride mask is reported. The optical feedback is provided by vertical as-grown crystalline facets. Double heterojunction lasers have been grown with this new structure and room-temperature operation has been achieved.

PACS numbers: 42.60.Jf, 42.82.+n

Integrated optical circuits (IOC's) will require a monolithic injection laser source which can be readily fabricated *in situ* in the IOC and will operate cw at room temperature. The development of such a localized laser source is crucial to the achievement of practical IOC's. Conventional semiconductor lasers with Fabry-Perot cavities formed by cleaving or polishing cannot satisfy this integration requirement. Distributed feedback (DFB) lasers[1-4] in which the optical feedback is provided by periodic gain and/or refractive index variation are a localized source. However, a DFB laser requires the fabrication of very short-period (~0.1 μm) gratings and the growth of the heterojunction structure is often a two-step process. Blum *et al.*[5,6] have reported a GaAs mesa structure in which the optical feedback is provided by vertical as-grown crystalline facets. This structure is grown by selective vapor phase epitaxy and can be used as a localized laser source. However, the mesas must be grown on (110)-oriented substrates [all IOC devices have been developed in (100)-oriented substrates] and, because of the difficult materials problems involved with this growth technique, only homojunction lasers have been fabricated.

In this paper we report a new localized mesa laser structure grown by liquid phase epitaxy. Vertical as-grown crystalline facets provide the optical feedback for the laser. The structure is grown on (100)-oriented substrates and is compatible with present IOC devices. Individual mesa lasers occupy only a small portion of a large GaAs substrate and we have grown arrays of several hundred mesas on a single chip. This method of fabricating lasers is compatible with the growth of complex layered waveguides and other electro-optic structures on the same chip. We have grown double heterojunction (DH) lasers with this structure and achieved room-temperature operation.

The substrates are (100)-oriented and polished GaAs wafers with n-type Si doping, $n \sim 3\times10^{18}$ cm^{-3}. Approximately 3000 Å of plasma-deposited silicon nitride are used to mask the substrate. Standard photolithographic techniques are used to define the pattern openings in the photoresist and a plasma etch opens the pattern in the silicon nitride mask. The window area is cleaned with a "common oxide" etch just prior to resist removal and placement in the growth system. The epitaxial layers are grown in a standard horizontal sliding graphite boat.[7] The starting growth temperature is 735 °C and cooling rates as slow as 0.1 °C/min have been used. The growth rate is greatly enhanced with masked substrates compared to unmasked substrates, and slow cool rates, short growth times, and low growth temperatures must be used to obtain reasonably thin layers. For the double heterojunction lasers four layers are grown: first, a Te-doped (~5×10^{17} cm^{-3}) $Ga_{0.7}Al_{0.3}As$ layer 3 μm thick; second, an "undoped" ($n \sim 5\times10^{16}$ cm^{-3}) GaAs active region 1 μm thick; third, a second $Ga_{0.7}Al_{0.3}$ 2 μm thick and doped with Ge (~2×10^{18} cm^{-3}); fourth, a final "cap" layer of Ge-doped GaAs (~5×10^{18} cm^{-3}) 1 μm thick for contacting.

The design of the laser device is constrained by device requirements and the limitations of selective liquid

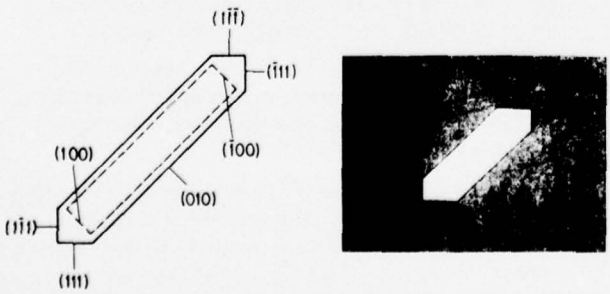

FIG. 1. Top view of a rectangular mesa oriented along ⟨100⟩ directions. (a) Dashed lines indicate the shape of the window in the silicon nitride mask. The solid lines represent the shape of the grown mesa. (b) A photomicrograph of the grown rectangular mesa. Note the perpendicular {100} facets along the long sides of the rectangle and the nonperpendicular {111} facets at the narrower ends.

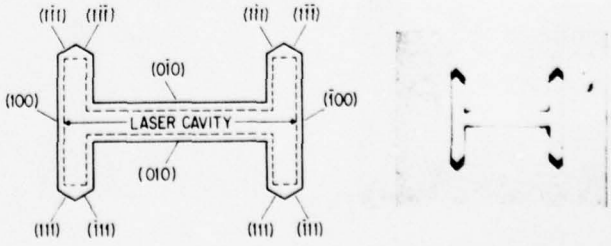

FIG. 2. Top view of the mesa laser grown on (100) GaAs substrate. (a) Dashed lines indicate the window opening in the silicon nitride mask. The solid lines represent the pattern of the grown mesa. (b) Photomicrograph of a grown I-bar mesa. Note the nonperpendicular facets at the ends of the cross bars.

phase epitaxy. The primary requirements are as follows: (1) facets perpendicular to the substrate to provide the optical feedback; (2) uniformly flat parallel epitaxial layers; (3) narrow stripe geometries. The first two requirements restrict the orientation of the device. The third requirement is necessary both for device performance (low operating currents) and to satisfy requirement (2) due to limitations of the growth process. Layer thicknesses become nonuniform for stripe widths greater than 25 μm. Samid *et al.*,[8] have shown that for (100) GaAs substrates stripes grown parallel to the (011) or (01$\bar{1}$) cleavage planes have facets which are not perpendicular to the substrate, and therefore, do not satisfy requirement (1). If we rotate the orientation of the opening 45° so that all sides are along the {100} planes, the structure shown in Fig. 1 results. The growth is a rectangular mesa with a flat top and facets perpendicular to the substrate along the long direction. However, the short ends are dominated by nonperpendicular {111} facets and the structure will not make a useful device. We have redesigned the rectangular structure as shown in Fig. 2 to yield the I-bar mesa laser. In this new structure the central member serves as the laser cavity region and perpendicular facets at the ends of the laser cavity provide the optical feedback. The nonperpendicular facets are moved out of the central cavity to the ends of the cross members. The length of the cross members have been exaggerated in Fig. 2 and must only satisfy the requirement of moving the nonperpendicular facets out of the central laser region. SEM photographs illustrating the high-quality as-grown facets are shown in Fig. 3. Typical I-bar dimensions are central laser cavity: 350–400 μm long, 25 μm wide; cross members: 150–350 μm long, 25 μm wide.

One of the principal advantages of the I-bar laser structure is the simplicity of device fabrication. Unlike conventional stripe geometry injection lasers that require fabrication steps such as proton bombardment[9] or selective diffusion[10] in addition to cleaving the individual devices, only p- and n-type contacts need to be affixed to the as-grown I-bars. The n-type contacts are made by electroplating Au-Sn to the substrate side of the wafer and alloying in a forming gas atmosphere

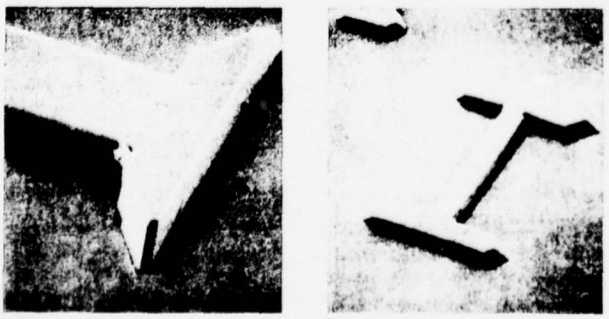

(a) (b)

FIG. 3. SEM photographs of the I-bar mesa laser. (a) A close-up of the end of the I-bar. The perpendicular crystalline facet provides the optical feedback for the laser cavity. (b) A full view of the mesa. Note the perpendicular sides and flat top except at the ends of the cross bars.

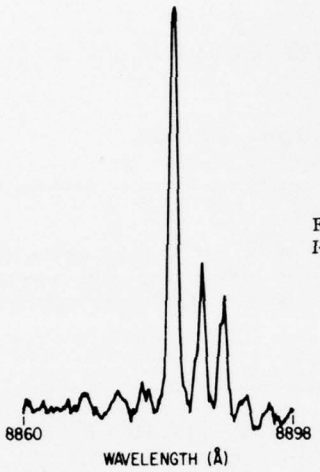

FIG. 4. Optical spectrum of an I-bar mesa laser.

at 500°C for 30 sec. Evaporated Cr-Au is used for the p-type contacts. As a result of the fact that the top p-GaAs layer surrounds the other layers and extends slightly over the silicon nitride growth mask, large area contacts extending well beyond the 15-μm-wide I bars can be used without shorting to the n-type layers. This facilitates bonding to the lasers. Usually, chips containing twelve I-bars are mounted to a transistor header for testing.

In the diode test apparatus, the devices are driven at a repetition rate of 500 pulses/sec with a 200-nsec pulse width. The light output is detected with an ITT FW 118 photomultiplier attached to a Spex $\frac{3}{4}$-m spectrometer. The room-temperature threshold current densities of initial devices typically have been less than 20 kA/cm^2. On lasers having an active layer thickness of approximately 1 μm the lowest threshold we have observed is 13 kA/cm^2. These devices exhibit the longitudinal mode spectra commonly observed for Fabry-Perot-cavity lasers. A typical spectrum is shown in Fig. 4. In the plane of the junction filaments are often observed indicating that these lasers are not operating in a single transverse mode. External differential quantum efficiencies have been measured with a calibrated PIN photodiode[11] and efficiencies as high as 15% have been observed. Although the device performance is not yet as good as conventional cleaved structures, there is no reason why these lasers should not perform as well or better than discrete lasers.

In conclusion, we have described a new type of monolithic double heterojunction laser grown by liquid phase epitaxy. These devices are useful laser sources for integrated optical circuits.

The authors are grateful to W. Abercrombie, P.K. Bunch, M. Howell, and S.S. Slingerland for skilled technical assistance. They wish to thank K.L. Lawley, R.E. Johnson, F.A. Blum, and J.T. Comfort for informative discussions and support.

* Work partially supported by the Office of Naval Research.

[1]K. Aiki, M. Nakamura, J. Umeda, A. Yariv, A. Katzir, and H.W. Yen, Appl. Phys. Lett. 27, 145 (1975).

[2]H.C. Casey, Jr., S. Somekh, and M. Ilegems, Appl. Phys. Lett. **27**, 142 (1975).
[3]M. Nakamura, K. Aiki, J. Umeda, and A. Yariv, Appl. Phys. Lett. **27**, 403 (1975).
[4]D.R. Scifres, R.D. Burnham, and W. Streifer, Appl. Phys. Lett. **27**, 295 (1975).
[5]F.A. Blum, K.L. Lawley, W.C. Scott, and W.C. Holton, Appl. Phys. Lett. **24**, 430 (1974).
[6]F.A. Blum, K.L. Lawley, F.H. Doerbeck, and W.C. Holton, Appl. Phys. Lett. **25**, 620 (1974).
[7]L.R. Dawson, J. Cryst. Growth **27**, 86 (1974).
[8]I. Samid, C.P. Lee, A. Gover, and A. Yariv, Appl. Phys. Lett. **27**, 405 (1975).
[9]J.C. Dyment, L.A. D'Asaro, J.C. North, B.I. Miller, and J.E. Ripper, Proc. IEEE **60**, 726 (1972).
[10]M. Takusagawa, S. Osaka, N. Takagi, H. Ishikawa, and H. Takanashi, Proc. IEEE **61**, 1758 (1973).
[11]E. Pinkas, B.I. Miller, I. Hayashi, and P.W. Foy, J. Appl. Phys. **43**, 2827 (1972).